# MULTI-ANTENNA DECOUPLING

AALBORG UNIVERSITY
Department of Electronic Systems
Mobile Communications 2009
10th Semester: Master Thesis

Majd Ali Irshaid

Daniel Pellitero Meseguer

**Antennas, Propagation and Radio Networking (APNet)**
**DEPARTMENT OF ELECTRONIC SYSTEMS**
Niels Jernes Vej 12
http://www.es.aau.dk/

---

**TITLE:** Multi-Antenna Decoupling

**PROJECT PERIOD:** The 10th Semester, February 2009 to May 2009

**PROJECT GROUP:** Mobile Communications Group 1114

**MEMBERS:**

Majd Ali Irshaid
Daniel Pellitero Meseguer

**SUPERVISORS:**

Gert Frølund Pedersen
Mauro Pelosi

*Abstract*

Nowadays, more data rate is being required in telecommunications, especially in mobile wireless communications. For this development, diversity systems like MIMO are being used, where multiple antennas are placed in the same handset. In order to achieve an optimum service, these antennas have to be designed properly taking in account important parameters. Some of these parameters are the mutual coupling, correlation and the total efficiency.

We design two planar inverted-F antennas (PIFAs) on a finite size ground plane representing the printed circuit board (PCB) of a typical mobile phone. We discuss several solutions to maximize the isolation and reduce the mutual coupling.

After designing the PIFAs for different frequency bands, we apply a hand to see how it effects on the whole system.

**PUBLICATIONS:** 3

**PAGES IN REPORT:** 39

**PAGES IN APPENDICES:** 30

**FINISHED:** 2 June 2009

# Preface:

This report is the outcome of our $10^{th}$ semester in Mobile Communication, carried out at the Department of Antennas, Propagation and Radio Networking (APNet), Institute of Electronic System at Aalborg University, Denmark.

This project is addressed to our supervisors, the teachers and students who are interested in the multi-antenna decoupling. The aim of this project is to document our $10^{th}$ semester work.

We would like to thank our project supervisors, Gert Frølund Pedersen and Mauro Pelosi, for their guidance and time throughout this project. We would also like to thank Mikael B. Knudsen from Infineon Technologies Denmark A/S. for his collaboration in this project.

Majd Ali Irshaid ________________

Daniel Pellitero Meseguer ________________

# Contents

# CHAPTER 1: Introduction

Wireless communication is rapidly increasing its demand for several high data rate applications. These several applications require better signal quality in both the terminal and the base station [1].

A solution to enhance the communication and its performance is to introduce a diversity system. This consists in integrating more than one radiating element in the terminal and also at the base station to generate a multiple-input multiple-output (MIMO) system. This solution is useful for a mobile handset as it is considered to operate in a multipath propagation environment where the electromagnetic field carrying the information will take several simultaneous paths between the transmitter and the receiver [2].

Nowadays, multiple antennas are needed to be integrated in the same handset as to support multiple standards such as UMTS band (1920-2170 MHz) or DCS1800 band (1710-1880 MHz). In mobiles normally the area allocated for the antennas is small with a limited available space. Therefore it is necessary to design properly the antennas of the handset and to take in account important parameters. Because changing the physical dimensions of the antenna will also affect on its efficiency and bandwidth [3].

When several antennas are placed in the same handset, there is an exchange of energy between them, this is called mutual coupling. The mutual coupling is one of the important parameters to take in consideration when designing an antenna. There are also more parameters which will be discussed during the report. Moreover, in the next section we define the problem we treat in our project which is how to reduce the mutual coupling.

## 1.1. Problem Deployment

As explained before, the main purpose of our project is to reduce the mutual coupling between the antennas without deteriorating other essential parameters for the mobile communication.

For the implementation of our project, we used planar inverted-F antennas (PIFA) explained in section 2.3. PIFA antennas are very practical antennas that can be designed for different standards, moreover; they are easily detuned when applying a hand. Compared to a monopole antenna, it has quite smaller dimensions at high frequencies [4].

The simulations and results for the investigation of the mutual coupling and the hand effects were done using a Finite-Difference Time-Domain (FDTD) code called AAU3 program written in Matlab high-level language developed at Antennas, Propagation and Radio Networking section, Department of Electronics Systems, Aalborg University, Denmark. Description of the FDTD method can be found in section 2.4.

During years, many studies were done to find techniques on how to reduce the mutual coupling and increase the isolation between antennas. One of these techniques was inserting a neutralizing line between the two PIFAs [5] [6]. Another technique was using an electromagnetic band gap structure (EBG). This EBG structure is introduced with an appropriate patch size and position [7; 8].

An important issue for mobile antennas is the human interaction with the antenna. There are several consequences when the human body is near the handset, such as radiation pattern deterioration, input impedance variation, detuning of the resonance frequency and absorption loss increase [9].

## 1.2. Report structure

The following parts of the report are structured in this way:

- *Background*: We explain some basic ideas of antennas, MIMO Systems and PIFAs.

- *Technical part*: We introduce our study for reducing the mutual coupling and the simulation results.

- *Conclusion*: We summarize the work done in this project and possible future works.

- *Appendix*: Description of some theorical background and basic simulations done for the complete understanding of this project.

The list of references, figures, tables are provided at the end of the report. The references are signed with square brackets during the whole report, e.g. [12]. The equations are marked with brackets taking in account the chapter number and the position of the equation in the chapter, e.g. (2.1) is equation number one of chapter two.

# CHAPTER 2: Background

## 2.1. Antenna

### 2.1.1. Definition

An antenna is a basic component in any communication system; it can be defined in many different ways. There are two types: the transmitter antenna and the receiver antenna. Normally the antenna is defined as a transmitter due to the reciprocity theorem (If the antennas and medium are linear, passive and isotropic, then the response of a system to a source is unchanged if the source and observer (measurer) are interchanged), as we know that the directional pattern of a receiving antenna is identical with its directional pattern as a transmitting antenna [10].

An antenna converts radio frequency fields into an induced current or vice-versa.

In Microwave Engineering [11], an antenna is defined as "*the component that converts a wave propagating on a transmission line to a plane wave propagating in free-space (transmission), or vice-versa (reception)*".

Various types of antennas have been developed up to this date, where each type is used depending on the system requirement. For mobile devices, PIFAs are commonly used. Explanations about PIFAs are found in section 2.3. Following we give a small description of some of the antenna parameters.

### 2.1.2. Antenna parameters

In this part as mentioned before, we explain briefly some basic characteristics of an antenna that are important to describe the performance of the antennas.

- **Radiation pattern**

From Antenna Theory [12] the radiation pattern of an antenna is defined as "*a mathematical function or a graphical representation of the radiation properties of the antenna as a function of space coordinates*".

The power received or transmitted by an antenna depends on its angular position and the radial distance from the antenna. So the variation of power density with angular position can be graphically represented as a radiation pattern plot commonly scaled in decibels (dB) [11]. It has different parts called lobes; the main, minor, side and back lobe. The lobes are regions with a certain intensity of radiation. The main or major lobe is the radiation lobe with the direction of maximum intensity radiation. The minor lobe is for any direction of radiation except the maximum one, i.e. any lobe except the major one. Usually represents undesired directions which therefore should be minimized. The side lobe is the adjacent lobe to the main lobe and normally is the largest of minor lobes. The back lobe is the radiation lobe with an axis that is 180° from the antenna beam [12].

There are different types of patterns depending if the antennas are: isotropic, directional and omnidirectional.

An isotropic antenna is defined in [12] as *"a hypothetical lossless antenna having equal radiation in all directions"*. This is physically not realizable but it is taken as a reference to express the directive properties of actual antennas. The directional antenna is also define in [12] as an antenna that has more efficient properties of radiating or receiving electromagnetic waves in some directions than in others. Finally an omnidirectional pattern has nondirectional pattern in a given plane and directional pattern in any orthogonal plane, i.e. it radiates or receives the same in all directions. It is a type of directional pattern.

- **Field regions**

The area around the antenna is divided in three regions. Depending in each region the field is structured in a specific way.

*Reactive near-field region*: it is the region where the near field exists at a distance of $R_1 < 0.62\sqrt{D^3/\lambda}$, which is the region immediately surrounding the antenna surface. Where *D* is the largest dimension of an antenna and $\lambda$ is the wavelength [12].

*Radiating near-field (Fresnel) region*: it is the field region between the reactive near field and the far-field. The distance is between $R_1 \geq 0.62\sqrt{D^3/\lambda}$ and $R_2 < 2D^2/\lambda$.

$R_1$ and $R_2$ are shown in figure 1.

*Far-field (Fraunhofer) region*: in this region the angular field is independent of the distance from the antenna. And the radiated wave has the form of a plane wave. The far field exists for distances farther than $R_2 > 2D^2/\lambda$. Radiation patterns are generally assumed to be in far-field of the antenna [12].

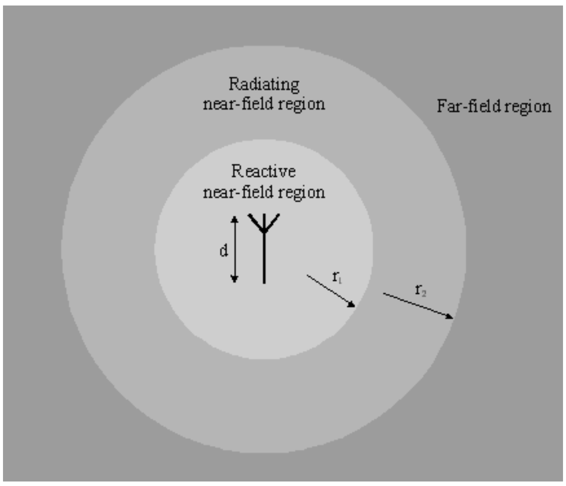


Figure 1: Field Regions [13]

- ### **Directivity**

Directivity is defined in [12] as *"the ratio of the radio intensity in a given direction from the antenna to the radiation intensity averaged over all directions"*. And the average radiation intensity as *"the total power radiated from the antenna divided by 4π"*.

$$D = \frac{U}{U_0} = \frac{4\pi U}{\mathrm{P_{rad}}} \qquad (2.1)$$

Sometimes it is desired to maximize the radiation direction of the transmitted or received power in a specific direction. The maximum value of this directive gain is the directivity of the antenna [11]. The directivity depends on the shape of the radiation pattern.

So if the direction is not specified, the maximum directivity is expressed as:

$$D_{\max} = \mathrm{D_0} = \frac{U_{\max}}{U_0} = \frac{4\pi U_{\max}}{\mathrm{P_{rad}}} \qquad (2.2)$$

- ### **Antenna Efficiency**

The total antenna efficiency takes in consideration the reflection, conduction and dielectric losses. The total efficiency is:

$$\mathrm{e_0 = e_r \cdot e_c \cdot e_d} \qquad (2.3)$$

Where:

$e_0$ is the total efficiency.

$e_r$ is the reflection efficiency due to the mismatch between the transmission line and the antenna.

$e_c$ is the conduction efficiency.

$e_d$ is the dielectric efficiency.

In [10] it is defined as *"the ratio of the total power radiated by the antenna to the input power of the antenna"*. Furthermore in section 2.2.3 we dedicate more explanations about the efficiency and its importance.

- ### **Gain**

It is an important parameter to describe the performance of an antenna. Takes in account the efficiency of the antenna and is related with the directivity. In [12] it is defined as *"the ratio of the intensity in a given direction to the radiation intensity that would be obtained if the power accepted by the antenna were radiated isotropically"*.

$$Gain = 4\pi \frac{radiation\ intensity}{total\ input\ (accepted) power} = 4\pi \frac{U(\theta,\emptyset)}{\mathrm{P_{in}}} \qquad (2.4)$$

We talk about different type of gains in section 2.2.4.

- **Impedance**

The input impedance of an antenna is the ratio of voltage (V) to current (I) at the antenna feed point

$$\mathrm{Zin} = \frac{V}{I} \text{ at the feed point} \qquad (2.5)$$

When there is more than one element, things change. For example the current distribution will not be the same and neither will be the field, as a result the input impedance also. This means we have to take in account the current of others element, therefore the mutual coupling. Mutual coupling is more detailed in section 2.2.1.

When the impedance is mismatched, this can degrade the antenna performance and as a result also its efficiency.

- **Bandwidth**

The bandwidth is *"the range of frequencies within which the performance of the antenna with respect to some characteristic, conforms to a specified standard"* [12].

Matching techniques can be used to increase the impedance bandwidth of an antenna [11] the impedance bandwidth is related with the input impedance and the radiation efficiency. In the other hand to relate the gain, polarization, side lobe level and beam direction it is referred to it as pattern bandwidth.

- **Polarization**

The polarization of an antenna is the polarization of the electric field of the transmitted or radiated wave by the antenna [12].

The polarization can be lineal (vertical or horizontal), circular and elliptical.

## 2.2. MIMO antenna system

MIMO refers to multiple-input and multiple-output, where multiple antennas are used in the transmitter and receiver due to the presence of multipath and scattering effects, such as fading "attenuation of the signal propagating through a certain media". Having more antennas helps the received signals to be more uncorrelated to each other.

MIMO's function is to produce significant capacity gains in respect with single input single output systems "SISO" using the same bandwidth and transmitted power [14].

Today high data rate is being demanded in wireless mobile communication. A handset is considered to be operating in a multipath scenario. This means that the electromagnetic field that carries the information will take many simultaneous paths between the transmitter and the receiver [5].

As mentioned previously a solution to this multipath problem is to place several antennas on the mobile terminal and also in the base stations. As a result, the communication performance can be enhanced by MIMO systems.

The antennas placed on the printed circuit board (PCB) must be designed properly considering important parameters such as the mutual coupling, the correlation, the total efficiency and the diversity gain.

In the following step we discuss each of the parameters.

### 2.2.1. Mutual coupling

When there are two antennas or more, these antennas transmit or receive power to each other. This depends on the distance between them, the radiation pattern and the orientation of each.

This interchange of energy on one of the antennas or on both may be rescattered in other directions permitting them to behave as second transmitters; this interchange of energy is called the mutual coupling [12].

The mutual coupling can be described with scattering "S" parameters.

The S-parameters can be found using the scattering matrix. The matrix relates the incident voltage waves in an N-port network with the reflected voltage waves [11].

The scattering matrix:

$$\begin{bmatrix} V_1^- \\ \vdots \\ V_N^- \end{bmatrix} = \begin{bmatrix} S_{11} & \cdots & S_{1\mathrm{N}} \\ \vdots & \ddots & \vdots \\ S_{\mathrm{N}1} & \cdots & S_{\mathrm{NN}} \end{bmatrix} \begin{bmatrix} V_1^+ \\ \vdots \\ V_N^+ \end{bmatrix} \tag{2.6}$$

If we want a specific element it can be found by:

$$S_{ij} = \frac{V_i^-}{V_j^+} \text{ With } V_k^+ = 0 \text{ for } k \neq j \tag{2.7}$$

What the formula says is that $S_{ij}$ is found by driving port *j* with an incident wave of voltage $V_j^+$ and measuring the reflected wave amplitude $V_i^-$ coming from port *i*.

### 2.2.2. Correlation

The correlation defines the independency between signals in the receiver. The correlation coefficient measures this independency where it varies from one and zero. When it is one it means total dependency between the signals [1].

The correlation and the mutual coupling have a direct relation. The lower the correlation is the lower is the mutual coupling. Therefore, when designing an antenna we require low mutual coupling as to obtain optimum diversity gain [6].

The correlation between signals in the receiver is important for the capacity of wireless communication in MIMO systems. For more capacity there has to be less correlation. But this is not always true, there are certain scenarios where the scattering is low around the transmitted and received antenna, leading to low correlated signals. Moreover there can be other propagation effects such as diffraction that result high scattering around transmitted and received antennas causing uncorrelated signals and as a result low capacity in the channel.

There are two type of antenna correlation: the signal correlation and the envelope correlation. The signal correlation is the correlation between complex signals and the envelope correlation is the correlation between amplitude signals received from different antennas. The envelope correlation is equal to the square of the complex signal correlation.

Hence, the correlation coefficient determines the quality of multichannel in the diversity and MIMO systems. The formula for the calculation of the correlation coefficient is:

$$\rho_{12} = \frac{|S_{11}^{*}S_{12} + S_{12}^{*}S_{22}|^2}{(1-|S_{11}|^2-|S_{21}|^2)(1-|S_{22}|^2-|S_{12}|^2)} \tag{2.8}$$

This formula has certain limitations in order to be valid [15]:

- The antenna system is positioned in a uniform multi-path environment.
- When the antenna port 1 is excited the other antennas are connected to the reference impedance.
- The antennas system has to be lossless structure, i.e. antennas of high radiation efficiency and no mutual losses.

Clearly the last point is not valid for our case. As the antennas have different type of losses, such as, losses due to the mismatching, losses due to the hand (dielectric losses) and losses of the metal.

The correlation of lossless is zero; this fundament is explained in most microwave books. For example it can be found in [11] which explain that the correlation coefficient is derived from the orthogonality between two signals coming from different antennas.

The correlation of loss is normally unknown and difficult to measure, so instead of assuming that it is equal to zero we consider it as an uncertainty [16].

The efficiencies have an effect on the correlation coefficient, for example, if both loss antennas have an efficiency of 50%, the uncertainty is ±1 considering that the correlation coefficient is within the unit circle. This uncertainty equals the largest distance of the unit circle; therefore this uncertainty is the limit of what can be said of an antenna beside the calculated from the S-parameters.

### 2.2.3. Total efficiency

The total efficiency is one of the most important considerations to take in account in a wireless communication.

The total efficiency of an antenna is defined as the total radiated power divided by the incident power at the feed. The efficiency is equal to the Mean Gain (MG), which is equal to the average antenna gain in the whole space [4].

Since we are dealing with antenna diversity and its performance, we define the Mean Effective Gain (MEG) as it is important for the environment in which the antenna is situated.

The MEG is a statistical measure of the antenna gain in a mobile environment. It is defined by the ratio between the mean received power of the antenna and the total mean incident power when moving the antenna over a random route [4].

### 2.2.4. Diversity Antenna Gain (DAG)

Is one of the most important parameters to evaluate the performance of diversity antenna. The DAG is defined as *DAG= MEG.DG* which can be considered as the gain system when it is compared to the reference antenna in the same propagation environment. DG is the Diversity Gain and can be defined as the improvement of signal to noise ratio (SNR) from combined signals from a diversity gain system with one single antenna in the system [4].

## 2.3. Planar Inverted F Antenna (PIFA)

An internal antenna increases the mechanical robustness of a mobile terminal. An internal antenna has limited bandwidth because of the size restriction; therefore it has to have a certain volume in order to have a good performance.

The PIFA is one of the main types of internal antennas for handsets, due to its compact size as it can be integrated into a handset. The PIFA reduces the power absorption to the head and it can be easily detuned when the user places its finger near the antenna elements. As there are more internal components in internal antennas it is harder to optimize them than external antennas [4].

Many promising PIFA designs for internal mobile phone antennas have recently been demonstrated, these designs are implemented with different type of arrangements.

The PIFA is a kind of linear inverted F antenna (IFA) with the wire radiator element replaced by a plate to expand the bandwidth [17].

- **Some advantages of using PIFAs are**:

    i. Its compact size where it can be hidden inside the handset.

    ii. The second advantage of the PIFA is that the backward radiation toward the user's head is being reduced, minimizing the Specific Absorption Rate (SAR) and enhance antenna performance.

    iii. The third advantage is the considerable gain in both horizontal and vertical states of polarization. This is useful in certain wireless communications where the antenna orientation is not fixed and the reflections are present from different corners of the environment, one of the important parameters of these cases is the total field, which is the sum of the horizontal and vertical state of polarization [17].

The resonant frequency of the PIFA is obtained by the following approximation:

$$F_{\mathrm{r}} = \frac{C}{4 \times (L_1 + L_2 + H - W)}$$

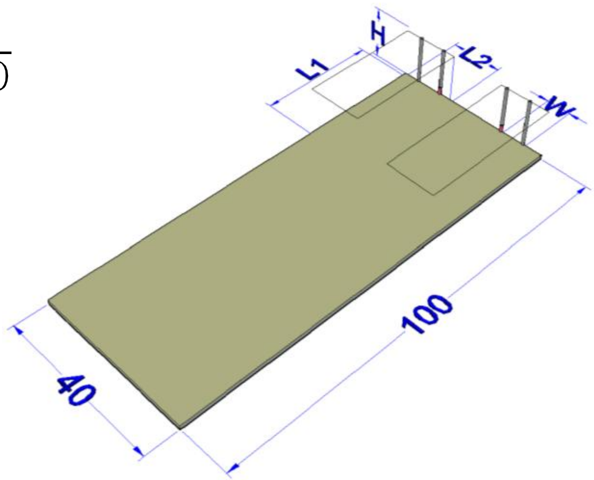


Where:

$F_r$ is the resonant frequency.

$C$ is light spread.

$L_1$ is the length of the PIFA.

$L_2$ is the width of the PIFA.

$H$ is the height of the PIFA.

$W$ is the distance between the feed strip and the short-circuit strip.

Introducing shaped slots to the PIFA reduces the frequency because of the existence of currents flowing at the edge of the slot.

PIFAs have larger current flows on the undersurface of the planar element and the ground plane than on the upper surface. Because of this, PIFAs are the best option when there is need to consider external objects that affect the antenna characteristics, e.g. the user's head or hand.

The impedance matching of a PIFA can be obtained by optimizing the distance between the feeding and shorting pins. Simulations where done and are found in appendix B. The main idea matching the PIFA is to abstain from adding lumped components as to avoid losses due to that.

The efficiency of a PIFA is reduced by all the losses suffered in it environment including ohmic losses, mismatching losses … etc

## 2.4. Finite-Difference Time-Domain (FDTD)

FDTD is used to calculate the fields. All the fields are initialized to zero. A source is introduced by setting a voltage at the feeding point and computing from it the electric field. The electric and magnetic field are calculated, the magnetic field at time $t = n + 1/2$ and the electric field is subsequently calculated at $t = n + 1$. Continuity of fields is enforced at a dielectric boundary in this algorithm. At the conductor interface the tangential electric field is zero. At the outer boundary Perfect Matched Layer (PML) is applied. Once the time domain is calculated, the frequency-domain quantities can be obtained from Fourier transforms.

The FDTD algorithm can be derived from Maxwell's equations. Further we show the way we used FDTD and how it is implemented in the simulator we used during this project. The simulator is explained in section 3.1.1.

The excitation source was placed in the Yee cell instead of one component of the electric component, as shown in the following figure:

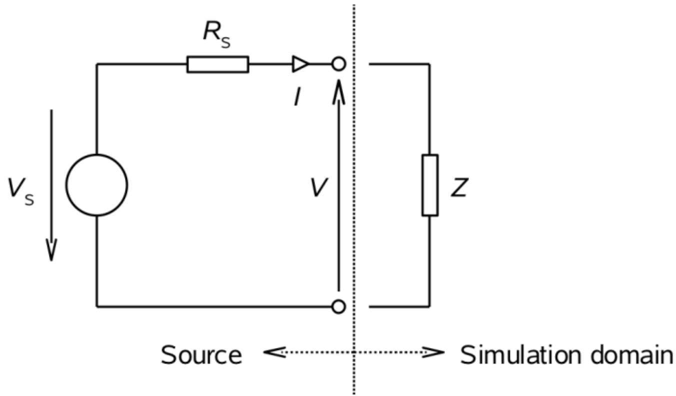


Figure 2: Excitation Circuit [18]

$V_s$ is the source voltage, $V$ is the input voltage, $R_s$ is the source impedance fixed to 50Ω and $I$ is the input current. The $V$ is obtained by the FDTD along the edge of Yee cell. It is calculated by this way:

$$I = \frac{V + V_s}{R_s} \tag{4.1}$$

Where the impedance Z is obtained by:

$$Z = -\frac{V}{I} = -\frac{R_S}{1+V_S/V} \qquad (4.2)$$

In the following figure, shows how the resistive source is added as a new branch in the E-field in Z direction.

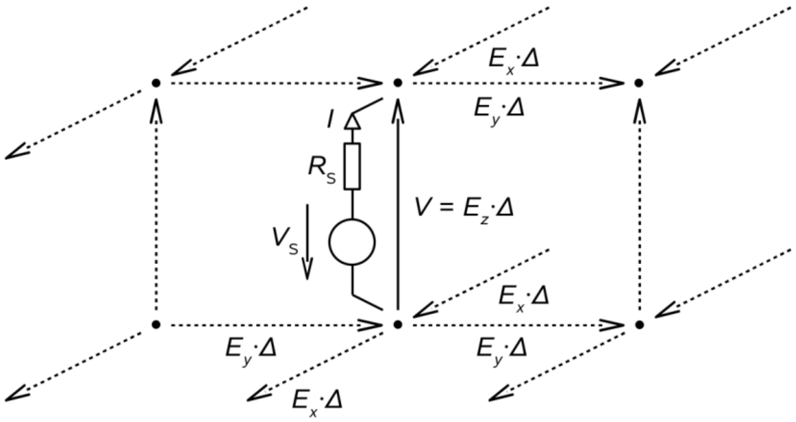


Figure 3: Yee Cell [18]

It is assumed a cubical Yee cell, i.e. the cell is homogeneous: $\Delta = \Delta x = \Delta y = \Delta z$.

From the differential form of Ampere's law:

$$\vec{\nabla} \times \vec{H} = \epsilon \frac{\partial \vec{E}}{\partial t} + \vec{J} \qquad (4.3)$$

Discretising by central differences in time instant $t = n + 1/2$ in Z direction as shown in figure X, we have:

$$\vec{\nabla} \times \overrightarrow{H^{(n+0.5)}} = \epsilon \frac{E_z^{(n+1)} - E_z^{(n)}}{\Delta t} + \frac{I^{(n+0.5)}}{\Delta^2} \qquad (4.4)$$

The total average is expressed in E-field and time averaging to fit in the time instant $t = n + 1/2$ :

$$I^{(n+0.5)} = \frac{E_z^{(n+1)} + E_z^{(n)}}{2} \cdot \frac{\Delta}{R_S} + \frac{V_S^{(n+0.5)}}{R_S} \qquad (4.5)$$

For $E_z$ field:

$$E_z^{(n+1)} = \frac{1-\frac{\Delta t}{2\epsilon R_S \Delta}}{1+\frac{\Delta t}{2\epsilon R_S \Delta}} E_z^{(n)} + \frac{\frac{\Delta t}{\epsilon}}{1+\frac{\Delta t}{2\epsilon R_S \Delta}} \vec{\nabla} \times \overrightarrow{H^{(n+0.5)}} - \frac{\frac{\Delta t}{\epsilon R_S \Delta^2}}{1+\frac{\Delta t}{2\epsilon R_S \Delta}} V_s^{(n+0.5)} \quad (4.6)$$

Where $R_s$ is the total value of conductivity in whole the Yee cell:

$$R_s = \frac{1}{\sigma} \frac{\Delta z}{\Delta x \Delta y} = \frac{1}{\sigma \Delta} \quad (4.7)$$

And the current density is:

$$J_{source}^{(n+0.5)} = \frac{1}{\Delta^2} \frac{V_s^{(n+0.5)}}{R_s} = \frac{I_s^{(n+0.5)}}{\Delta^2} \quad (4.8)$$

For the frequency domain, Discrete Fourier Transform (DFT) is used. The input voltage (or the input current) is saved as a sequence of samples in time which are transformed in frequency domain by FFT algorithm with the following relation:

$$\Delta t \cdot \Delta f \cdot N_t = 1 \quad (4.9)$$

Where $\Delta t$ is the time steps, $N_t$ is the number of samples and $\Delta f$ is the frequency resolution [18].

# CHAPTER 3: Simulations & Results

## 3.1. Simulations

To investigate the mutual antenna decoupling system we used a simulator deployed at Aalborg University called AAU3 with the help of the supercomputer *Fyrkat*.

Thanks to *Fyrkat*, we were able to save a lot of time in executing our simulations. Simulations without *Fyrkat* take more time (e.g. various days) and are less accurate. More information of *Fyrkat* can be found in [19].

We give a small description of how the simulator works.

### 3.1.1. Simulator

The simulator AAU3 is based in FDTD method, explanations can be found in section 2.4. There are two possibilities to run the simulations: either by Matlab Kernel or by Fortran Kernel. Fortan kernel spends less time than Matlab kernel. The interface of the simulator; written in Matlab, is where the input parameters are inserted and where the geometry of the system is designed. This interface is essential to get the results of the simulation like plots or numerical parameters.

Before running the simulation we have to take a look at the simulator´s input parameters and adapt them to the scenario which we want to simulate. Most of these parameters belong to the FDTD method. These parameters are essential to take in consideration when figuring out the results obtained. Further information is found in the manual of the AAU3 [18].

The scenario of the simulations is based on one or two antennas (dipoles, monopoles and PIFAs) placed on top of a small ground plane whose size represents the Printed Circuit Board (PCB) of a typical mobile handset. The dimensions of the PCB are 100x40 mm. An example can be shown in the following figure:

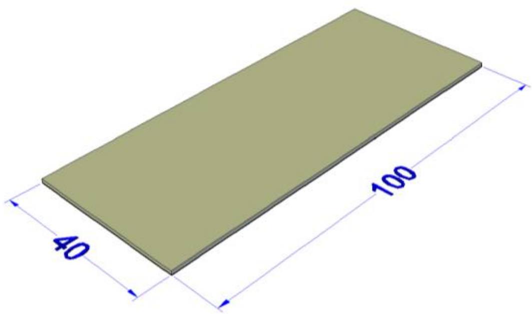


Figure 4: PCB

- **Explanations:**

We assume that our scenario is an isotropic network; therefore $S_{21}$ is equal to $S_{12}$. Moreover in further results we only show $S_{21}$ as they are the same.

The $S_{21}$ values of the graphs are the highest peak of the wave in the both used bands of frequency (DCS and UMTS), i.e. the worst situation looking at the $S_{21}$.

## 3.2. Results

For the understanding of some basic principles of the mutual coupling, we firstly did simulations on dipoles. The simulations consisted in designing the dipoles at different frequencies and later changing the distances from each other. From the results found in Appendix B, we noticed that when two dipoles are not close in frequency, e.g. one dipole at 900 MHz and the other at 1800 MHz, the mutual coupling is less than the case when the two dipoles are at the same frequency. We also did simulations on typical monopole antennas for a mobile handset. Results can be found in Appendix B.

The second step consisted in gaining knowledge on how to design PIFAs. The dimension of the PIFA was designed using the approximation in Section 2.3.

We introduced several arrangements in the dimensions, the height, the distance between feeding strip and short circuit strip…etc. These arrangements helped us develop and match the PIFAs for our needed requirements. The simulations of these arrangements were done for the frequency of 1800 MHz.

Some of these arrangements are:

- *Changing the distance between feeding strip and short circuit strip (W):*

We redesigned the PIFA with different *W* preserving the rest of the dimensions. From this we realize that when increasing the distance between the feed strip and the short circuit strip, the frequency increases to a higher one. This can be shown in graph 5 (it can also be found in Appendix B):

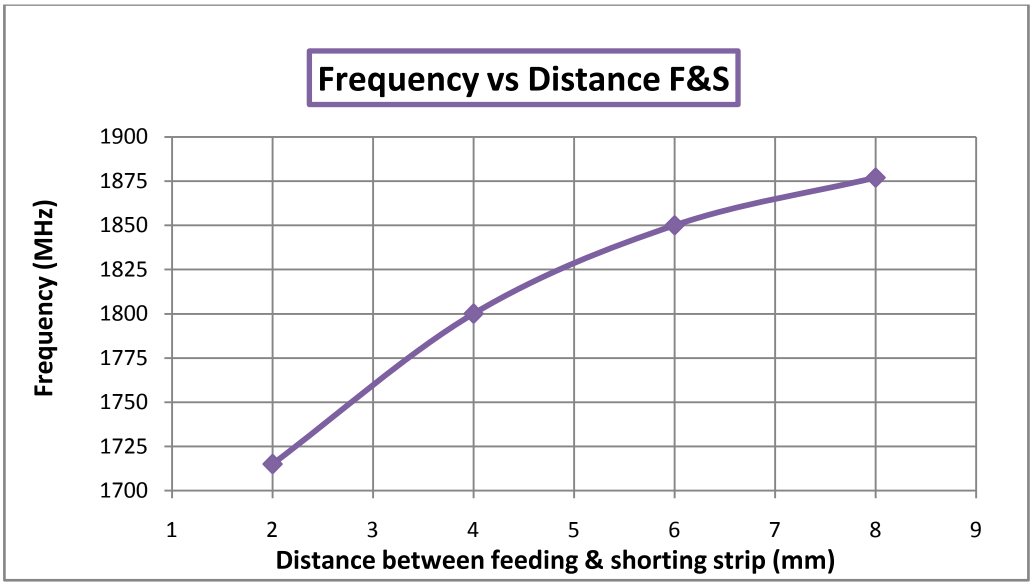


Figure 5: Frequency vs. Distance between feed strip & short circuit strip

➢ *Changing the height of the PIFA (H):*

Here we redesigned the PIFA as in the previous point, except that we redesigned it for different heights (*H*), beginning from 5 mm till 10 mm. As a result, the resonant frequency decreases and the impedance increases with the height.

Comparing it to the first arrangement when varying the *W*, we observe that in this case when varying the height, the frequency shift is higher. How the frequency changes with the height is in figure 6.

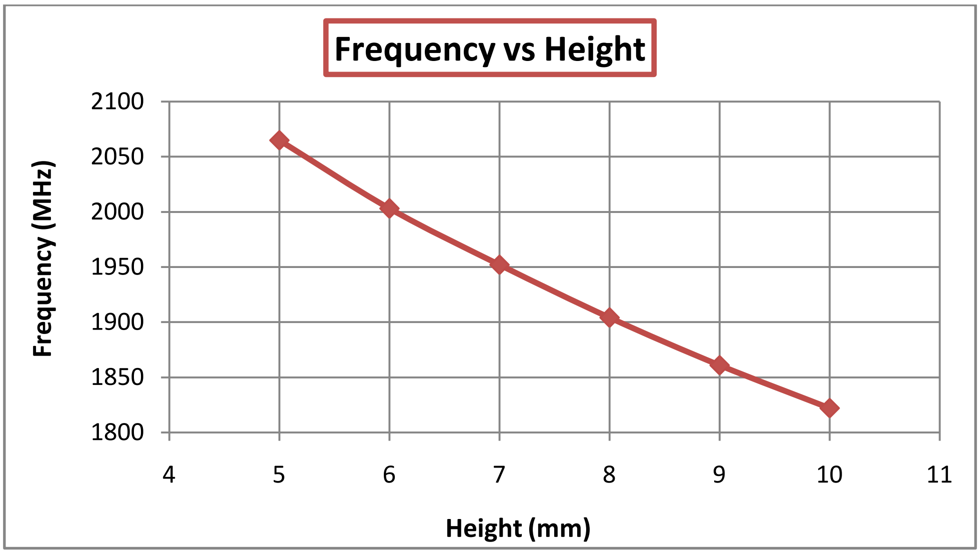


Figure 6: Frequency vs. Height of PIFA

For the impedance, we can see that the impedance at resonant frequency changes depending on the height of the PIFA. How the impedance varies with the height is shown in the figure above:

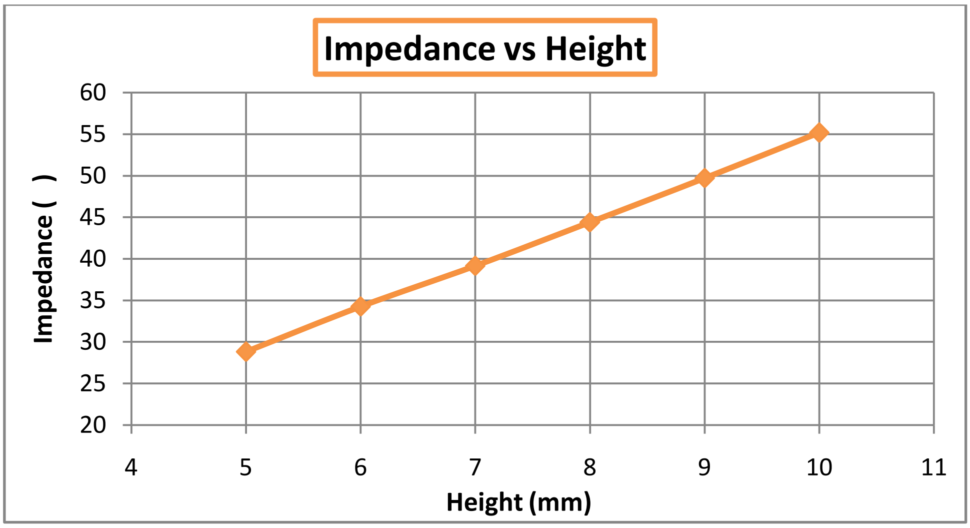


Figure 7: Impedance vs. Height of PIFA

Further details are found in Appendix B.

### 3.2.1. Two PIFAs

We placed two PIFAs on the same PCB to investigate the mutual coupling. The PIFAs are designed in close frequencies such as, for DCS [1.71-1.88 GHz] and UMTS [1.92-2.17 GHz] bands. At the beginning, as with the dipoles, we looked at the variation of the $S_{21}$ in respect with the distance between the antennas. Then we studied scenarios with different positions of the PIFAs on the PCB. We also simulated among these scenarios, the facing of the feeding strip and the circuit shorting strip. As in figures above:

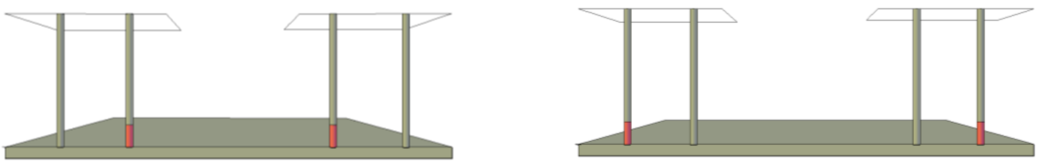

Figure 8: Feed facing configuration (left) & short facing configuration (right)

Mostly the short facing configuration give us better mutual coupling “$S_{21}$” in respect to the feed facing configuration.

In the end, mainly we designed one PIFA for DCS and the other PIFA for UMTS. So in further simulations the PIFAs used, are in these same frequency bands.

More investigations about different scenarios for PIFAs are in Appendix B.

### 3.2.2. Dielectric Simulations

As a solution for reducing the mutual coupling, we thought of inserting ceramic materials, i.e. dielectric materials with high permittivity and low loss. The dielectric material is introduced in the antenna (PIFAs) scenario in several ways.

Initially we used a dielectric wall with different permittivities ($\varepsilon_r$ =10, 30, 50, 70, 100). This dielectric wall was placed in the middle of both PIFAs. The width of this wall is 2mm with a height of 10mm and a length of 50mm. As mentioned previously, one PIFA is designed for DCS band and the other PIFA is designed for UMTS band.

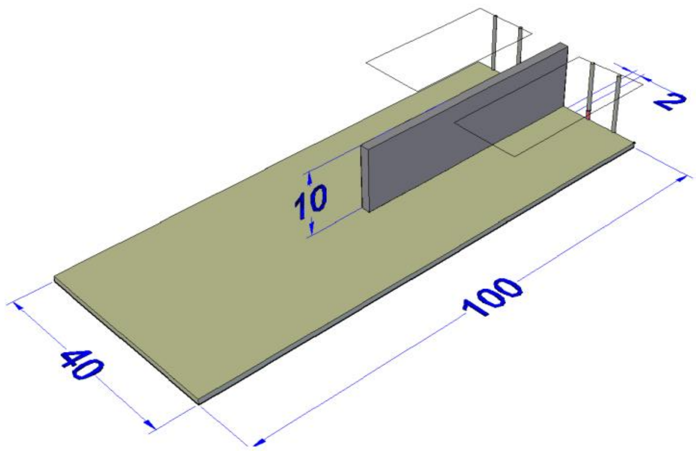


Figure 9: PIFAs with one dielectric wall

At first sight of simulation results, we observe that there is an alteration in the design of the PIFAs comparing it to the configuration without dielectric wall (free space). Therefore we redesign the PIFA so as when inserting the dielectric wall, we obtain a matched PIFA at the desired frequency. Redesigning the PIFA consists in reducing the PIFA´s size.

Introducing a dielectric wall we notice that we get some improvement in the $S_{21}$. Hence we continue our research by inserting two dielectric walls.

The Scenario of two dielectric walls is represented in figure 10.

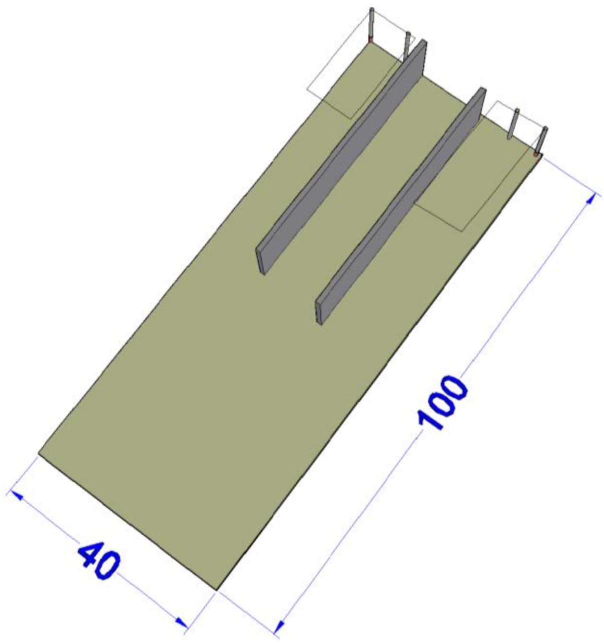


**Figure 10: PIFAs with two dielectric walls**

The width of the two dielectric walls is 2mm at a height of 10mm and a length of 50mm. We studied two different configurations for this case:

- *The Vertical PCB configuration (V):* (Shown Figure 10)
- *The Horizontal PCB configuration (H):*

**Figure 11: Horizontal PCB configuration (H)**

In this case the distance between the PIFAs is longer than the vertical case.

As done for one dielectric wall, we investigated using dielectrics with different permittivities. The results gained were better than the configuration of one dielectric wall.

- *Our results are*:

In this graph, we can see how the $S_{21}$ of the different configurations varies depending on the permittivity of the dielectric walls. As explained before, the $S_{21}$ values of this graph are the highest peak of the wave in both used bands of frequency (DCS and UMTS).

If we take a look at the graph, we notice that the $S_{21}$ is lower in permittivities from 80 to 100 than when there is no dielectric wall applied. More information about the exact values is in Appendix B.

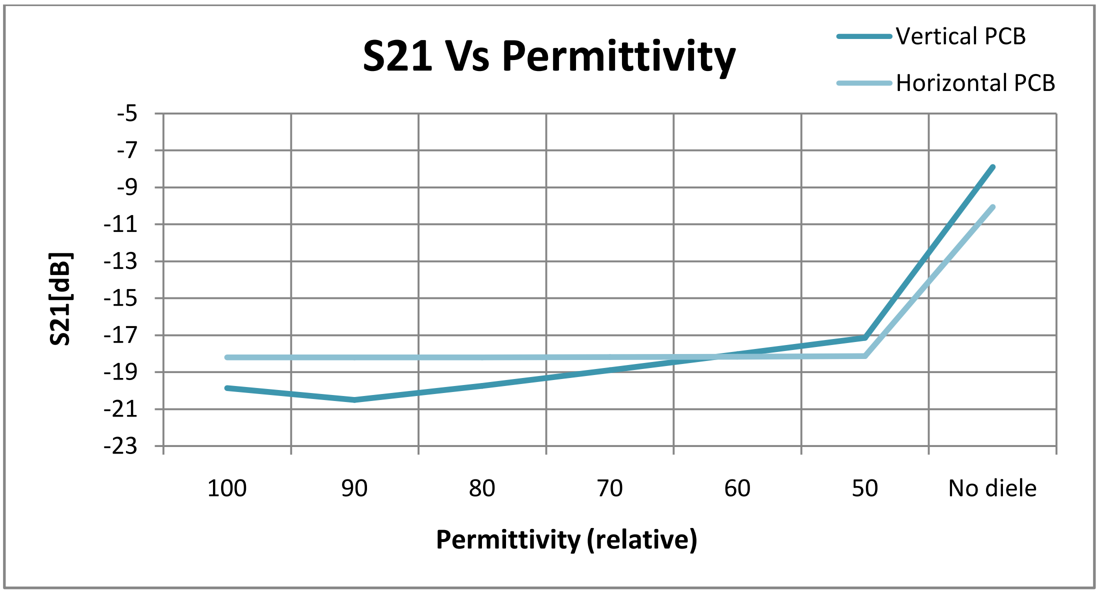


**Figure 12: S21 vs. Permittivity of the wall**

In the next graphs, we compare the total efficiencies of the different configurations. The total efficiency was calculated by the following formula:

$$\eta_{tot} = \eta_{ray}(1 - |S_{11}|^2 - |S_{21}|^2) \qquad (3.1)$$

Where $\eta_{tot}$ is the total efficiency and $\eta_{ray}$ is the radiation efficiency.

Comparing different configurations results, we see from graph 13 that the total efficiency in V configuration is more sensible to the change of permittivity than the H configuration. This can be due to the separation between the two PIFAs.

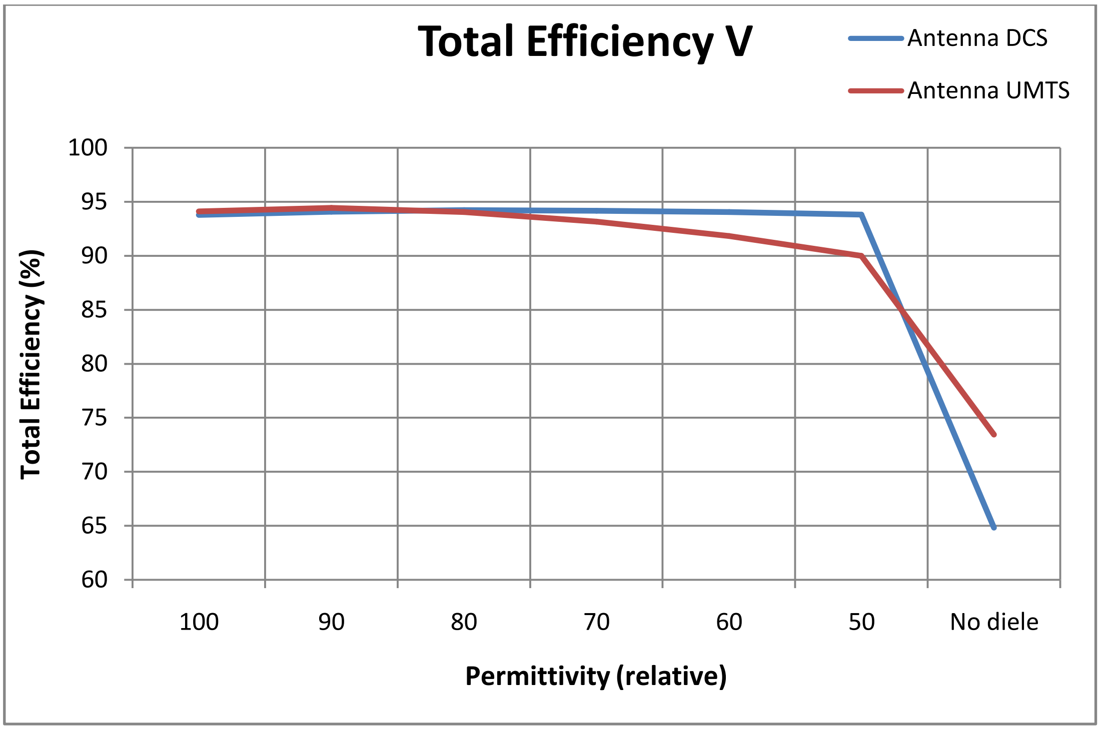


Figure 13: Total efficiency for vertical configuration (V)

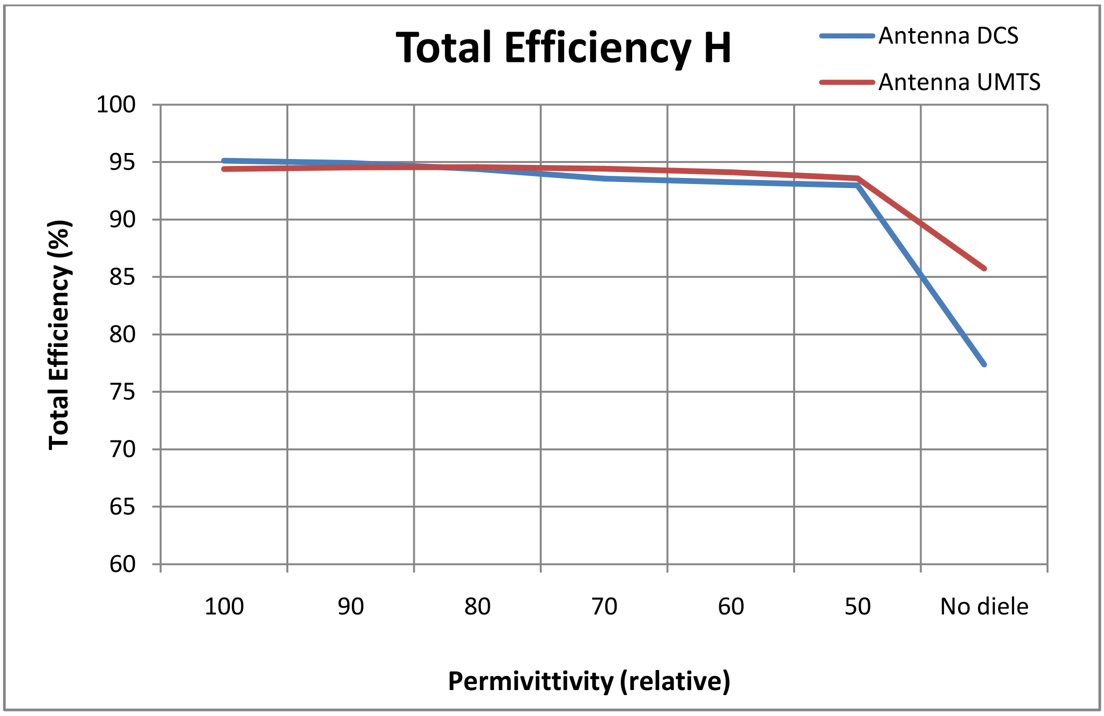


Figure 14: Total efficiency for horizontal configuration (H)

Later when applying the hand, we perceive more differences between these two configurations. The results will have more variations compared to each other, as what can be seen in the next part.

Until now all the dielectric materials used in the simulations where without conductivity, for an approximation to reality we searched for a dielectric material with the following characteristics:

A permittivity of $\varepsilon_r$= 103.1 and a loss tangent of $tg(\delta)$= 0.0088.

The conductivity was calculated from the following formula:

$$tg(\delta) = \frac{\sigma}{w \varepsilon_r \varepsilon_0} \qquad (3.2)$$

Where $\sigma$ is the conductivity (*S/m*), $w$ is equal to $2\pi f$ (*rad/s*) and $\varepsilon_0$ is the permittivity in free space equal to 8.85$* \ 10^{-12}$ (*F/m*) and $\varepsilon_r$ is the relative permittivity.

In the figure below, we show the results with and without conductivity in the dielectric material. $S_{11}$ and $S_{22}$ do not have much variation but $S_{21}$ has a small deterioration, also does the radiation efficiency which decreases its value around 2%.

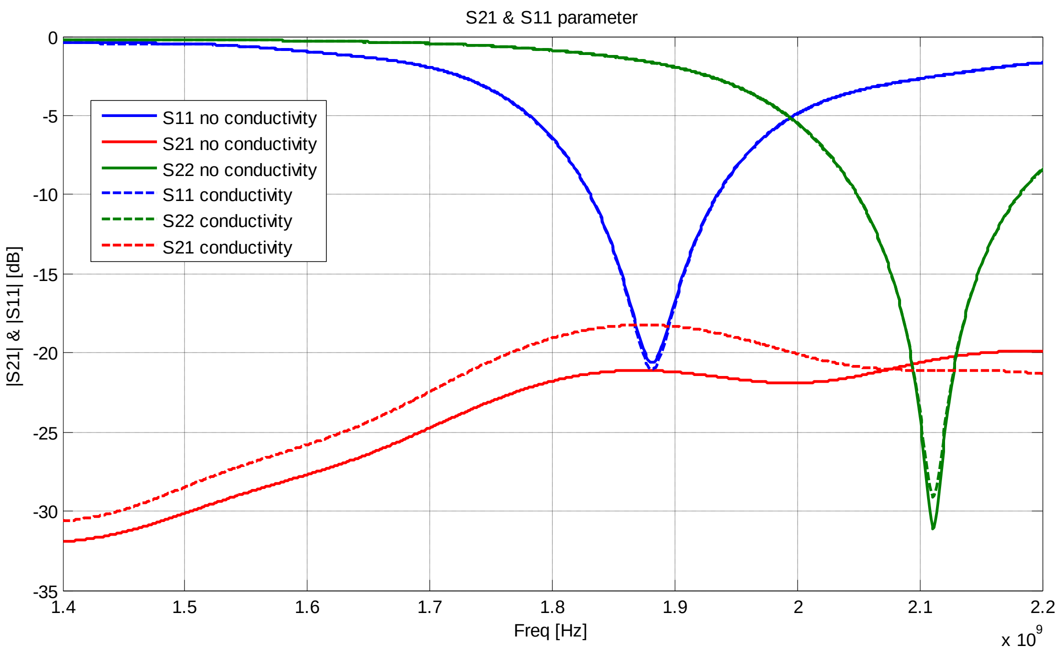


**Figure 15: Conductivity vs. no Conductivity**

### 3.2.3. Results with hand

After designing the PIFAs and inserting the dielectric walls in free space, it is time to make it closer to real life. This can be achieved by adding a hand.

We use six different hand models provided by our supervisor Mauro Pelosi. The shape of the hands models are scaled to a hand anthropometric study [20]. The dielectric compositions of the hands are defined according to the study in [20]. For example, for 1800

MHz the hand has $\varepsilon_r$ equal to 32.6 and $\sigma$ equal to 1.26 *S/m*. There are two types of hand grips: the soft grip and the firm grip. The difference between both grip styles is the gap between the palm and the handset. In the firm grip the gap is smaller than the soft grip [21].

The table above describes briefly the type of hands and the position of the index finger. We look at the orientation of the hand as holding the mobile handset in a usual grab.

| Type of Grip | Hand Number | Index Position |
|---|---|---|
| FIRM GRIP | Hand 1 (h1) | Right |
| | Hand 2 (h2) | Middle |
| | Hand 3 (h3) | Left |
| SOFT GRIP | Hand 4 (h4) | Right |
| | Hand 5 (h5) | Middle |
| | Hand 6 (h6) | Right |

In V configuration the DCS PIFA is on right side of the PCB and the UMTS PIFA is on the left side. So when hands 1 or 4 are applied the index finger is on the DCS PIFA on the other hand, when hands 3 or 6 are applied the index finger is on the UMTS PIFA.

For H configuration we decided to place the index finger on the DCS PIFA and the palm of the hand on the UMTS PIFA. Hands 1 and 4 in this configuration are somehow touching the part of the PIFA where the feeding strip and the short circuit strip are. However hands 3 and 6, touch the side of the PIFA where there is nothing connected, i.e. in the other part of the PIFA.

An important point to take in account is that the gap between the index finger and the height of the PIFAs is **3 mm**.

Below we show examples of the different hand models with their different grips on V configuration and H configuration. More examples on hands are in Appendix C.

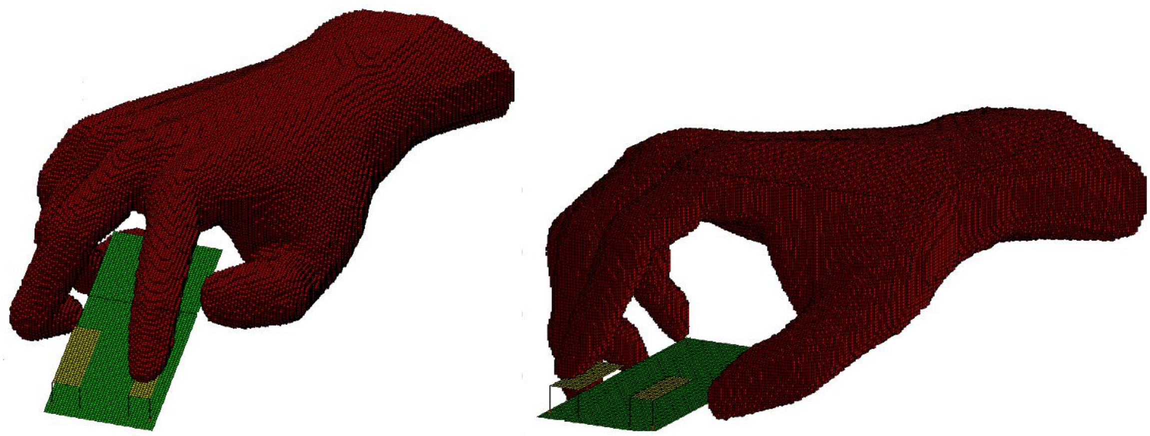

Figure 16: Hand 3 (left) & Hand 4 (right) with V Configuration

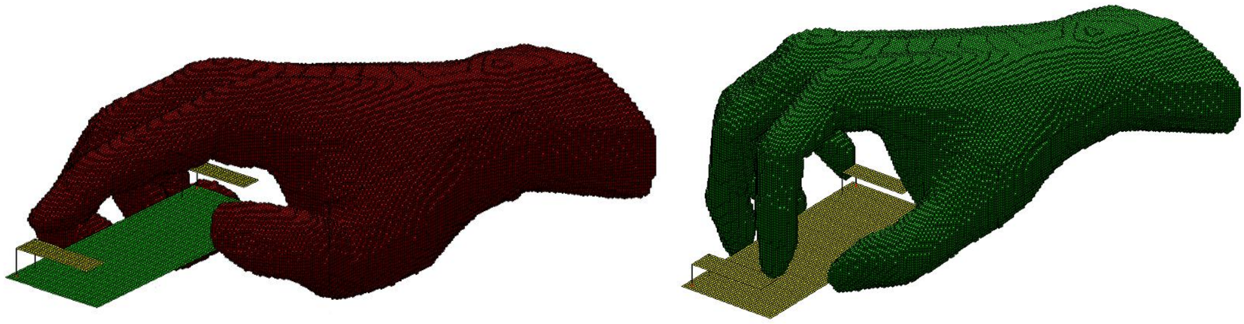

Figure 17: Hand 1 (left) & Hand 6 (right) with H configuration

After executing various simulations, these are the results obtained (in order to see the table with values go to Appendix B):

The dielectric walls used in these simulations are of $\varepsilon_r = 100$ and $\sigma = 0.09\ S/m$.

In the results we evaluate the absorption loss and the mismatch loss:

$$Absorption\ loss = Radiation\ Efficiency\ (dB)$$

$$Mismatch\ loss = 10\log_{10}(1 - |\rho|^2)\ where\ \rho = S_{11}\ (lineal)$$

## ➢ Vertical configuration (V)

*a) Vertical configuration (V) with different hands:*

Here we only have the two PIFA antennas without any dielectric walls.

As shown in the Figure 18, with hand 1 & 4 the DCS antenna has more absorption loss comparing to the UMTS antenna. This is due to that the index finger is touching the DCS antenna. When the index finger touches the antenna the absorption loss increases [9].

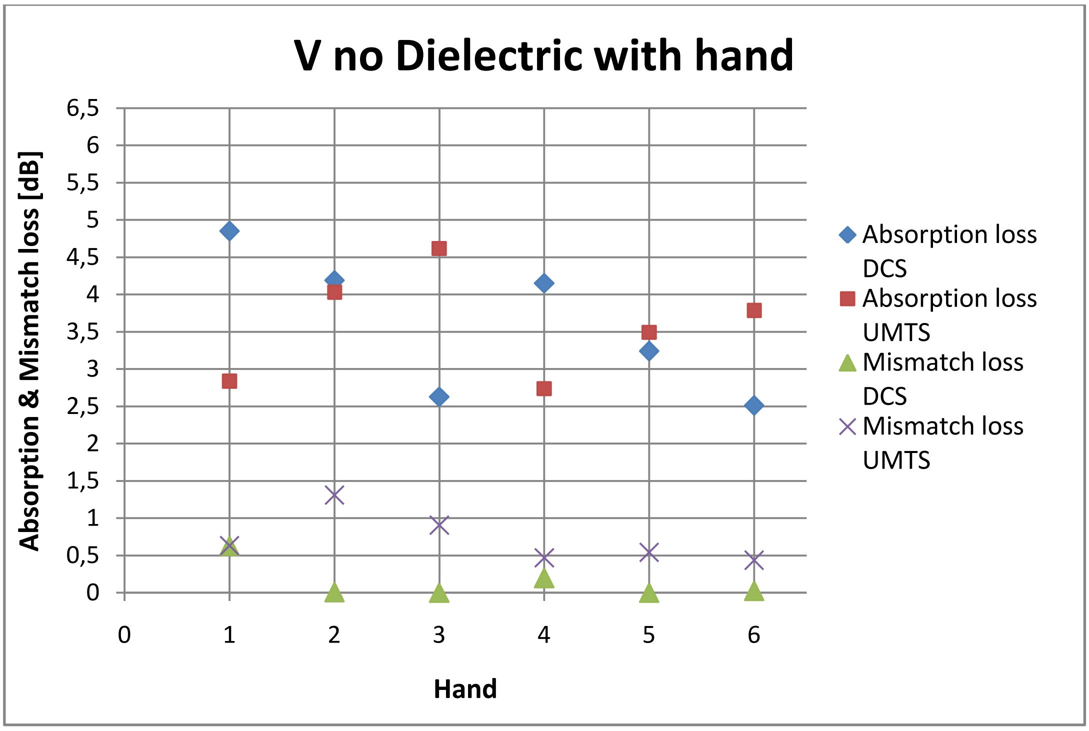


Figure 18: Absorption loss for Vertical configuration (V) without dielectric wall

*b) Vertical configuration (V) with two dielectric walls & different hands:*

The dielectric walls used are the ones explained in the previous section.

In this case with the two dielectric walls, the absorption and mismatch losses decrease compared to the case where the V configuration was without dielectric walls.

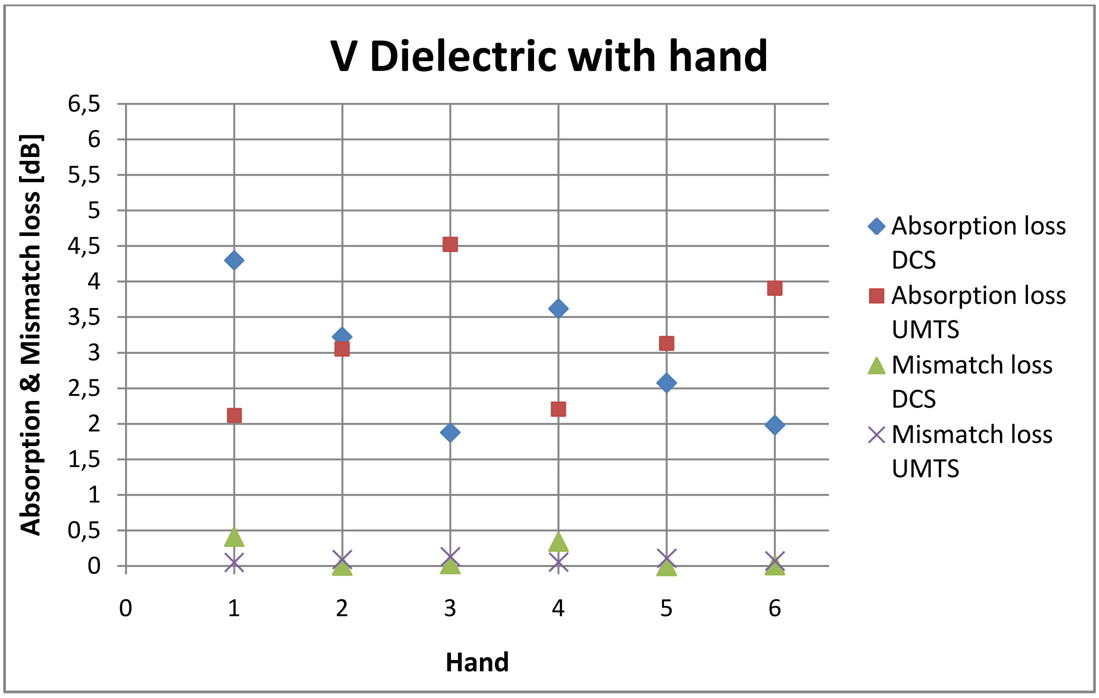


Figure 19: Absorption loss for Vertical configuration (V) with two dielectric walls

## ➢ Horizontal configuration (H)

*a) Horizontal configuration (H) with different hands:*

For this configuration, the hand has the index finger on top of the DCS antenna and the palm on the UMTS antenna. Therefore when the hand is firm grip; both losses are higher in UMTS antenna than in DCS antenna. This is because the palm has more losses than the index finger. Besides, we can notice that the soft grip has less loss than the firm grip for both antennas, this is due to the firm has smaller gap between the palm of the hand and the handset [9].

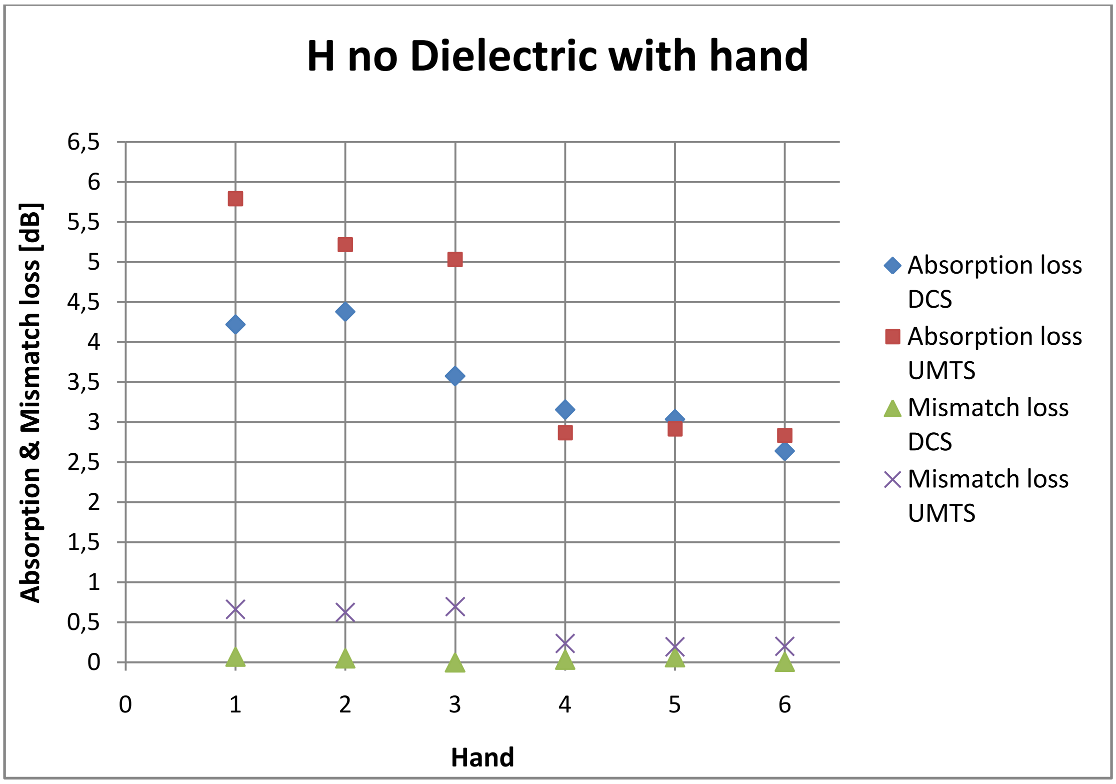


Figure 20: Absorption loss for Horizontal configuration (H) without dielectric wall

*b) Horizontal configuration with two dielectric walls & different hands:*

The explanation of these results is the same as the one explain for V configuration with two dielectric walls. We realize that the palm-handset gap has strong influence on both losses but because of the dielectric walls there is a small improvement on them.

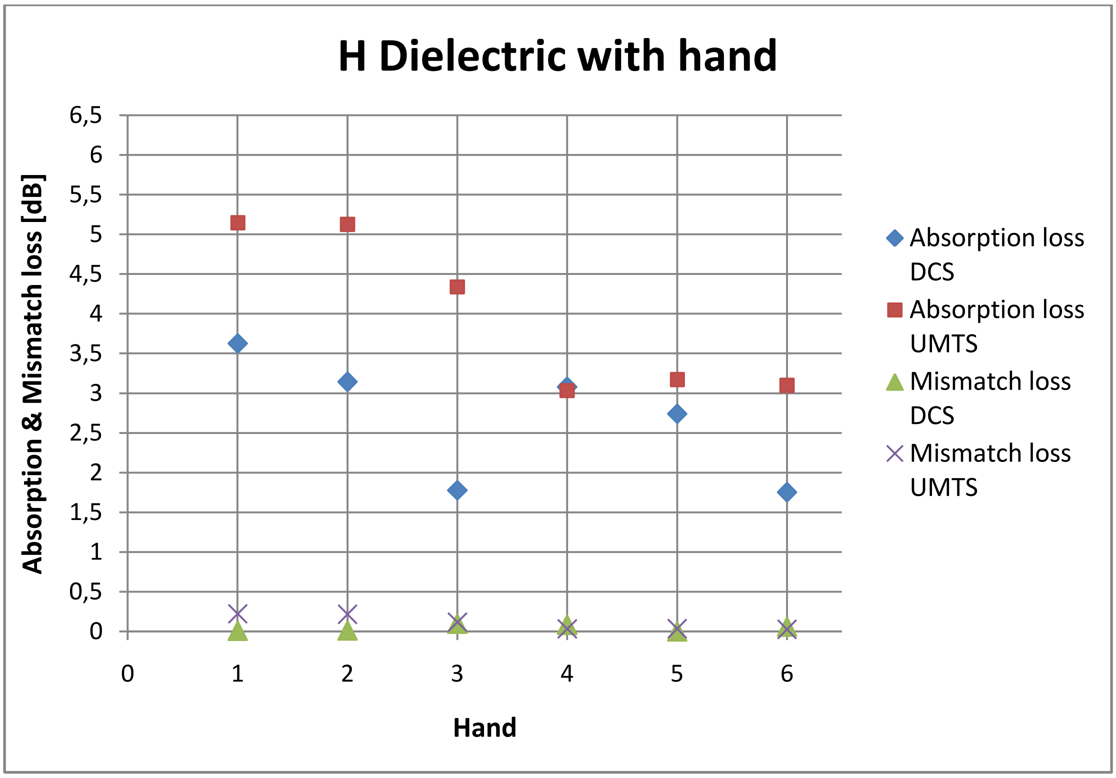


Figure 21: Absorption loss for Horizontal configuration (H) with two dielectric walls

- **Total Efficiency**

In this part we compare the total efficiency of each antenna in the different configurations mentioned before to see which one has better performance.

For DCS antenna, it has similar results in both configurations (V & H), except that for hands 1 & 4, the H configuration has around 7% better total efficiency than the V configuration.

The worst total efficiency is when no dielectric walls are introduced.

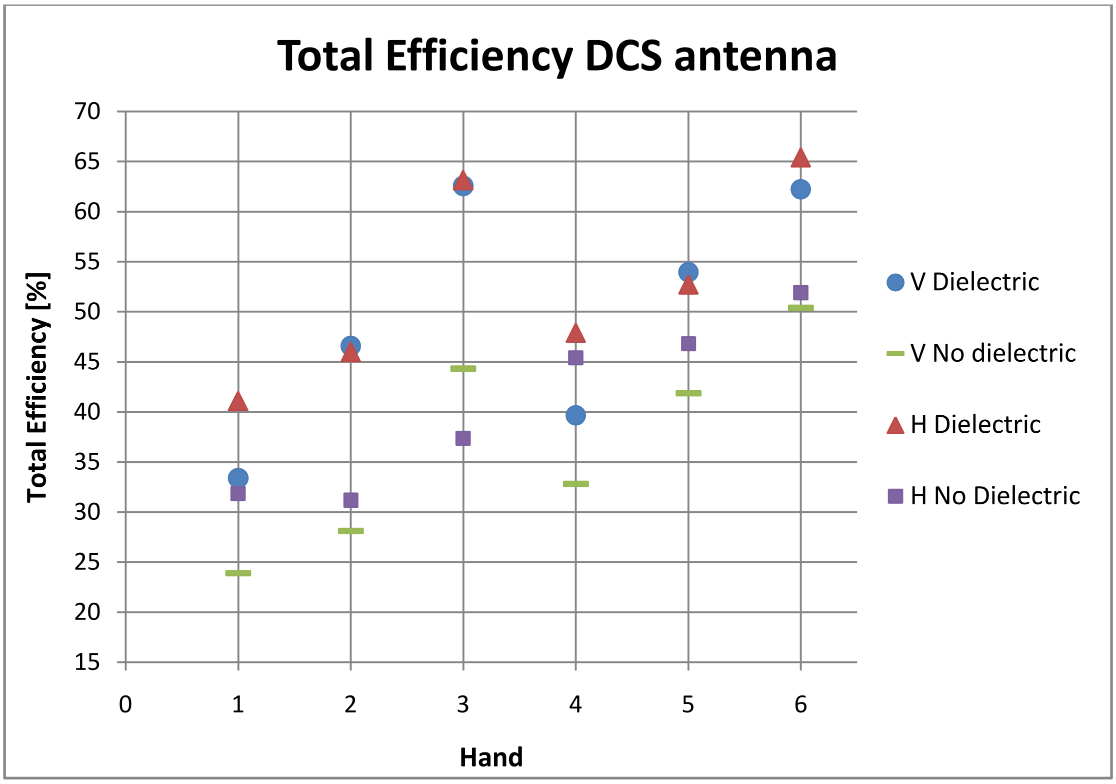


Figure 22: Total Efficiency for DCS antenna

The total efficiency of UMTS is better for V configuration in firm grip style. As when it is in H configuration the palm is on top of the UMTS antenna region. On the other hand, using the soft grip styles with dielectric walls or not, does not really affect on the total efficiency as there is more gap between the palm and the handset.

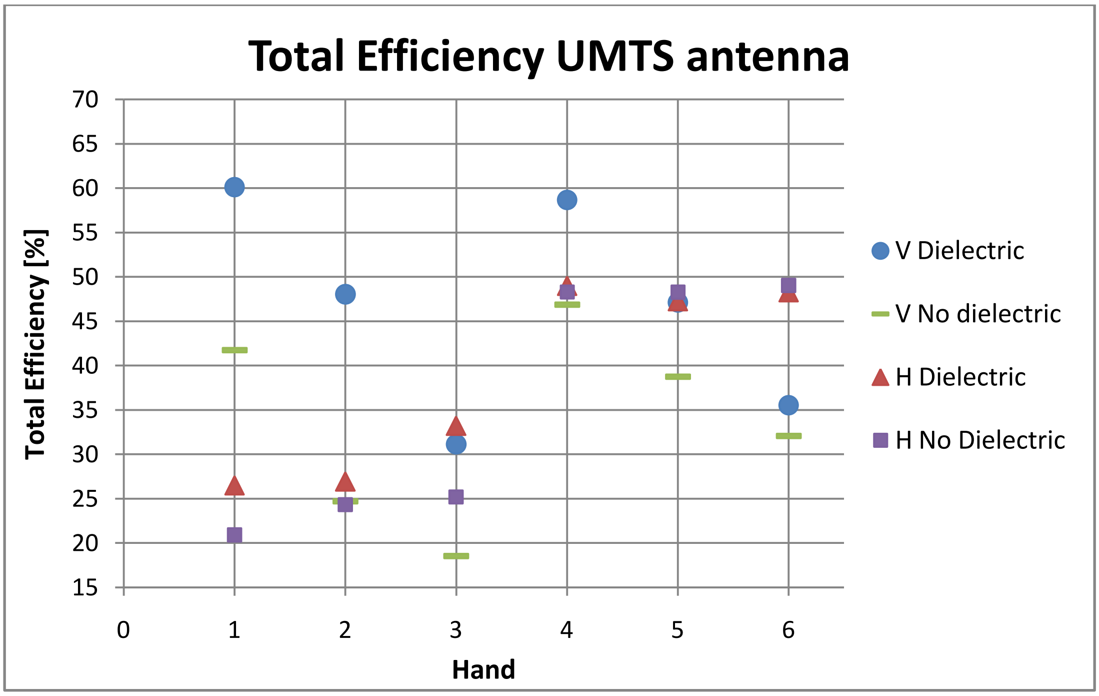


Figure 23: Total Efficiency for UMTS antenna

# CHAPTER 4: Conclusions

In this chapter, the general conclusions carried out through this project are presented. In addition, we propose several ideas for future works.

## 4.1. What we have done

The basic goal of this project was to investigate a novel way to achieve a diversity antenna system in a mobile handset having in mind the important parameters such as the mutual coupling that lead to obtain an optimum performance.

Firstly, we studied some basic antennas such as dipoles and monopoles to understand how the system of two antennas work and the way the $S_{21}$ changes depending on different circumstances. We designed the dipoles for 900 MHz and 1800 MHz, creating different scenarios by placing these two dipoles at many distances.

Secondly, our next step was to get ourselves familiar with the PIFA antenna. We designed the PIFAs at different resonant frequencies being able to match them. Various scenarios were built changing the height of the PIFA from the PCB, the distance between feeding strip and short circuit strip, separation between PIFAs and placing them on different positions on top of the PCB. These scenarios were applied for one or two PIFAs. Doing all of this we managed to gain a view of what would be the ideal configuration for PIFAs.

Thirdly, we searched for works done on this area, where several techniques for reducing the mutual coupling were found. We obtained a brief guidance for finding a mean to reduce the mutual coupling. We simulated some of these previous investigations exactly to check if we were able to obtain the same results and learn why they were capable to enhance the isolation. Simulations on [6] are in Appendix D.

Finally after all this work, the idea of inserting a dielectric material was applied. This was encouraging because we think that a dielectric material can be adapted to the handset's size, also due to its cost and the easy implementation with the simulator. Our simulations began with inserting a dielectric wall in between the two PIFAs and then we inserted two walls instead of one, as it can be seen in the previous chapter. The final step was to see if the results were robust when applying the hand.

## 4.2. Future Works

One possible improvement is to find a way in making the system more robust when applying a hand. This may be achieved by adding a substrate and a superstrate to the PIFAs [3].

The work done during this project can be held in real implementation so as to take measurements to prove the simulated results or to help in enhancing them.

Our investigations with dielectrics were upon PIFAs in DCS and UMTS bands, other bands can be treated for further investigations such as GSM 900 (Global System for Mobile communications). We investigated for PIFAs of 900 MHz using the same scenario of this project but we did not gain considerable results. More work can be done with 900 MHz PIFAs and multi-band antennas.

Finally, reducing the mutual coupling with dielectric walls is a wide investigation where more design configurations can be studied, for instance a multilayer dielectric wall configuration.

# List of Figures

# Bibliography


1. *Project Presentation 2009.*

2. *Channel Capacity Evaluation of UMTS Multi-Antenna Systems in Indoor And Outdoor Environments.* **A. Diallo, C. Luxey, P. Le Thuc, R. Staraj, G. Kossiavas, P. Suvikunnas,M. Mustonen.** 11-16 Nov.2007, page(s): 1-5.

3. **Mauro Pelosi, O. Franek, Mikael B. Knudsen, Gert Frølund Pedersen.** *Influence Of Dielectric Loading on PIFA Antennas in Close Proximity with the User´s Body.*

4. **Fujimoto, Kyohei.** *Mobile Antenna Systems Handbook.*

5. **A. Chebihi, A. Diallo, C. Luxey, P. Le Thuc,R. Staraj.** Optimization of the neutralization technique to enhance the diversity performance of a two-antenna system for UMTS mobile phones. *Antenna Technology: Small Antennas and Novel Metamaterials, 2008.* 4-6 March 2008, page(s): 522-525.

6. **A. Diallo, C. Luxey,P. Le Thuc, R. Staraj, G. Kossiavas,.** Study and Reduction of the Mutual Coupling Between Twp Mobile Phone PIFAs Operating in the DCS1800 and UMTS Bands. Nov. 2006, Vol. 54, 11, page(s): 3063-3074.

7. **Fan Yang, Yahya Rahmat-Samii.** Mutual Coupling Reduction of Microstrip Antennas Using Electromagnetic Band-Gap Structure. 2001, Vols. 2,page(s): 478-48.

8. —. Microstrip Antennas Integrated With Electromagnetic Band-Gap (EBG) Structures: A Low Mutual Coupling Design For Arrays Applications. Oct. 2003, Vol. 51, 10, page(s): 2936-2946.

9. **Mauro Pelosi, O. Franek, Mikael B. Knudsen, Gert Frølund Pedersen.** Antenna Proximity Effects for Talk and Data Modes in Mobile Phones.

10. **Johnson, Richard Clayton.** *Antenna Engineering Handbook.*

11. **Pozar, David M.** *Microwave Engineering.*

12. **Balanis, Constantine A.** *Antenna Theory: Analysis and Design.*

13. www.giangrandi.ch/electronics/anttool/regions.gif. [Online]

14. http://users.ece.utexas.edu/~rheath/research/mimo/antenna/. [Online]

15. **A. Diallo, C. Luxey, P. Le Thuc, R. Staraj and G. Kossiavas.** Enhanced two-antenna structures for universal mobile telecommunications system diversity terminals. *IET Microwaves, Antennas & Propagation.* February 2008, Vol. 2, 1, p. 93-101.

16. **Hallbjorner, P.** The significance of radiation efficiencies when using S-parameters to calculate the received signal correlation from two antennas. *IEEE Antennas and Wireless Propagation Letters.* 2005, Vols. 4, page(s): 97- 99.

17. http://www.qsl.net/va3iul/. [Online]

18. **Franek, Ondrej.** AAU3 The 3rd Generation FDTD Code version 0.3.6. *Antennas, Propagation and Radio Networking Department of Electronic Systems, Aalborg University.*

19. http://presse.aau.dk/nyheder/3353908. [Online]

20. **Mauro Pelosi, O. Franek, Gert Frølund Pedersen.** Influence of Tolerances in Homogeneous Material Properties of Hand Phantoms.

21. **Mauro Pelosi, O. Franek, Mikael Knudsen, Morten Christensen, Gert Frølund Pedersen.** A Grip Study for Talk and Data Modes in Mobile Phones. *IEEE Transactions on Antennas and Propagation.* Vol. 57, 4, pp. 856-865.

22. **Steven G. Johnson.** Notes on Perfectly Matched Layers (PMLs) . [Online] July 19, 2008.

23. **Taflove, Allen.** *Computational Electrodynamic The Finite Difference Time Domain Method .*

24. **A. Diallo, C. Luxey, P. Le Thuc, R. Staraj, G. Kossiavas,M. Franzen.** MIMO performance of enhanced UMTS four-antenna structures for mobile phones in the presence of the user's head. *Antennas and Propagation Society International Symposium, 2007 IEEE.* 9-15 June 2007, Page(s):2853 - 2856.

# Appendix A. Glossary

## I. Abbreviations

DAG: Diversity Antenna Gain
DCS: Digital Cellular System
DFT: Discrete Fourier Transform
DG: Diversity Gain
EBG: Electromagnetic Band Gap
FDTD: Finite Difference Time Domain
GSM: Global System for Mobile communications
H configuration: Horizontal configuration
MEG: Mean Effective Gain
MG: Mean Gain
MIMO: Multiple-Input Multiple-Output
PCB: Printed Circuit Board
PIFA: Planar Inverted-F Antenna
PML: Perfect Matched Layer
SNR: Signal to Noise Ratio
UMTS: Universal Mobile Telecommunications System
V configuration: Vertical configuration

## II. Definitions

- **Specific Absorption Rate (SAR)**

Is one of the parameters to discuss related to health risk caused by the interaction between the human with the mobile antenna.

SAR is a value that measures how much power is absorbed in biological tissue when the body is exposed to electromagnetic radiation [4].

The SAR is defined as:

$$SAR = \frac{\sigma}{\rho}|E|^2 \; [W/kg]$$

Where E is the electric field (V/m),$\sigma$ is the conductivity (S/m) and $\rho$ is the density ($Kg/m^3$).

Spatial-peak SAR is defined as the maximum average SAR of a 10g or a 1g cubic volume of tissue.

The ANSI/IEE standard C95.1-1992 RF Safety Guideline suggests that the 1g averaged peak SAR should not exceed 1.6 W/Kg and the whole body average peak-SAR should be less that 0.08 W/Kg [4].

- **Perfect Matched Layer (PML)**

Is an artificial boundary layer designed to absorb outgoing waves from the interior of the computational region without letting them reflect back to inside the computational region. This is commonly used to truncate the computational domain with an artificial boundary layer. PML was initially derived for electromagnetism of Maxwell's equations but now it is used to other wave equations [22].

- **SNR**

It is the power ratio of the desired signal to the undesired noise. This ratio is normally measured in dB.

- **Yee Cell**

It is a representation of how the Yee algorithm centers it E and H components in three-dimensional space. Where every E component is surrounded by four H circulating components and every H component is surrounded by four E circulating components [23].

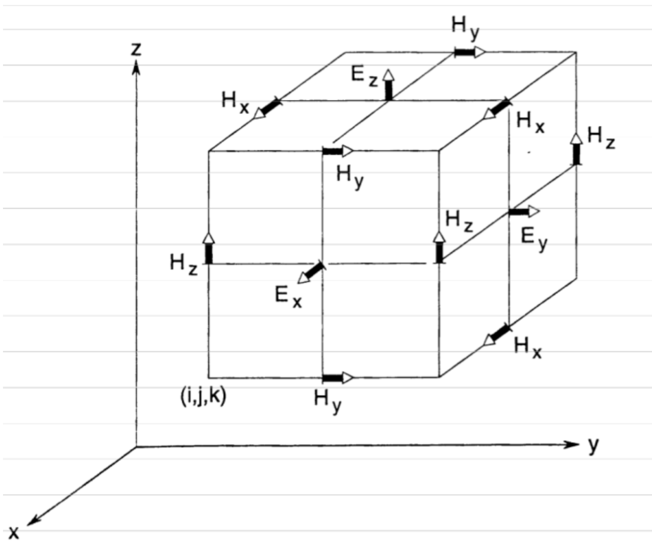


Figure 24: Yee Cell [23]

# Appendix B.

## I. Dipoles

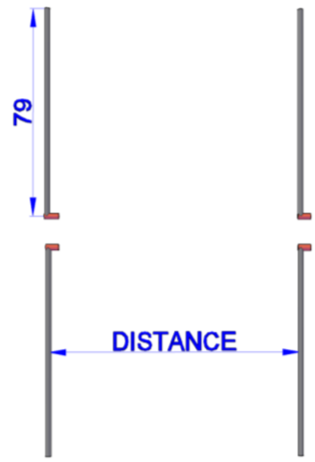


- **Design of the dipoles**
  - Dipole $\lambda/2$ of $f$ =900Mhz:

    $\lambda = \frac{c}{f} \rightarrow \lambda$ =1/3 m where $\lambda$/2=1/6m (79mm+79mm)
  - Dipole $\lambda$ /2 of $f$ =1800Mhz:

    $\lambda$ =1/6 m where $\lambda$ /2=1/12m (39mm+39mm)

- **Two dipoles at 900 MHz. separated d= 1mm, 6mm, 10mm, 15mm and 20 mm.**

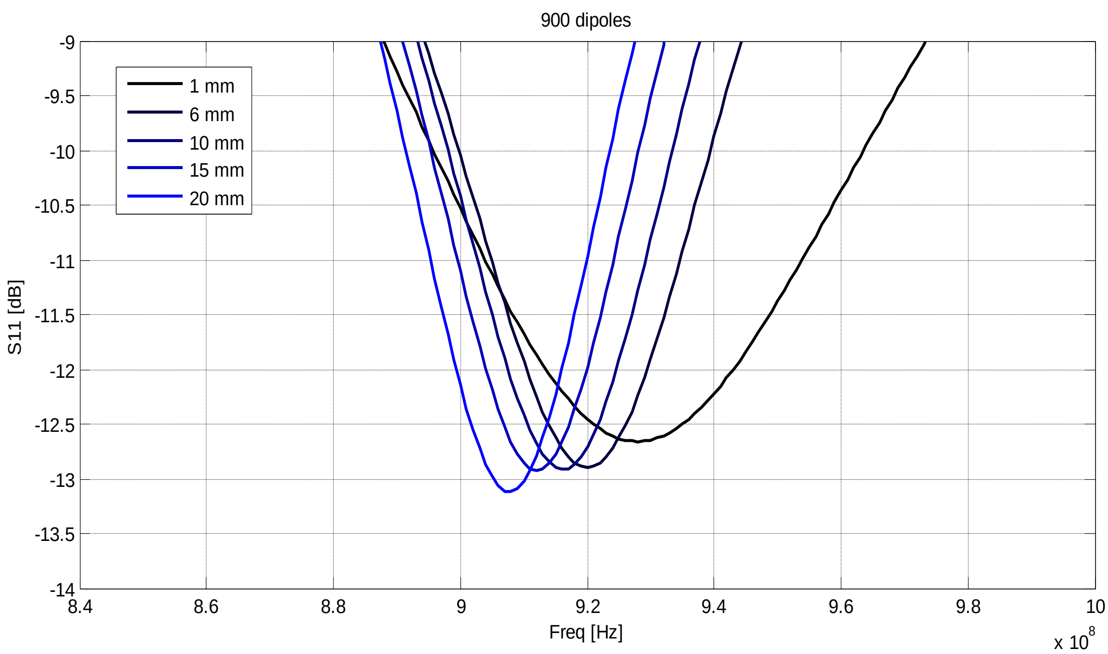


Figure 25: S11 & S22 dipoles 900MHz

We can notice that with higher separation between the dipoles, the closer it is to the designed frequency and it has better $S_{21}$. The following graph shows how $S_{21}$ changes with the distance.

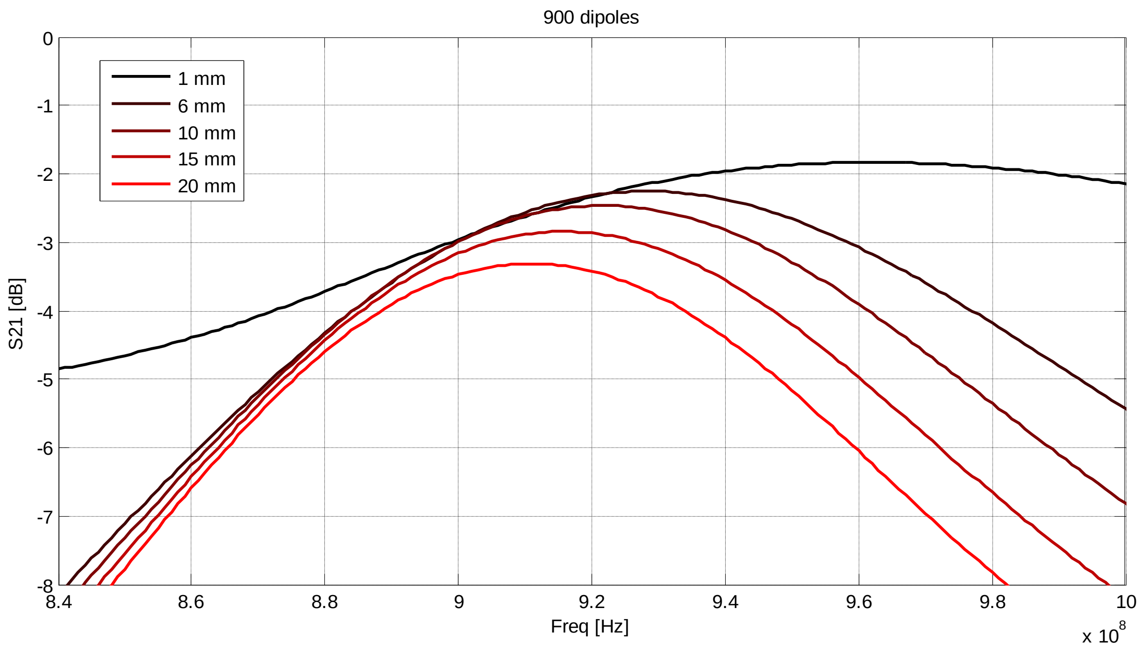


Figure 26: S21 dipoles 900 MHz

- **Two dipoles at 1800 MHz separated d= 1mm, 6mm, 10mm, 15mm and 20 mm.**

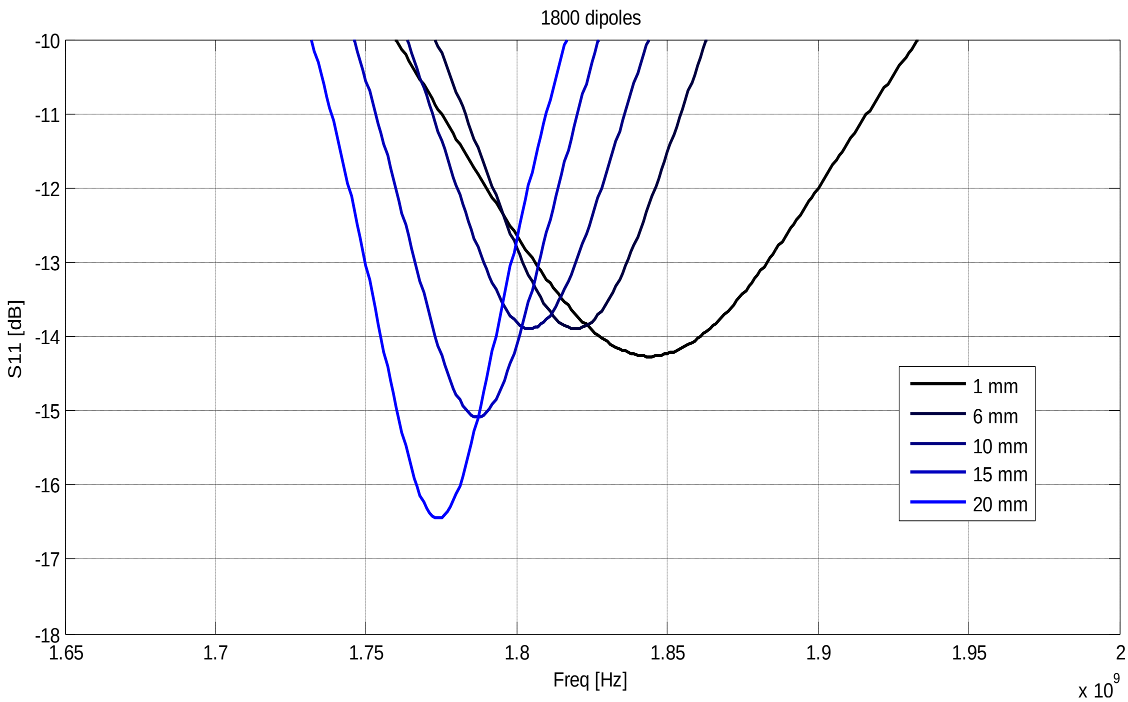


Figure 27: S11 & S22 dipoles 1800 MHz

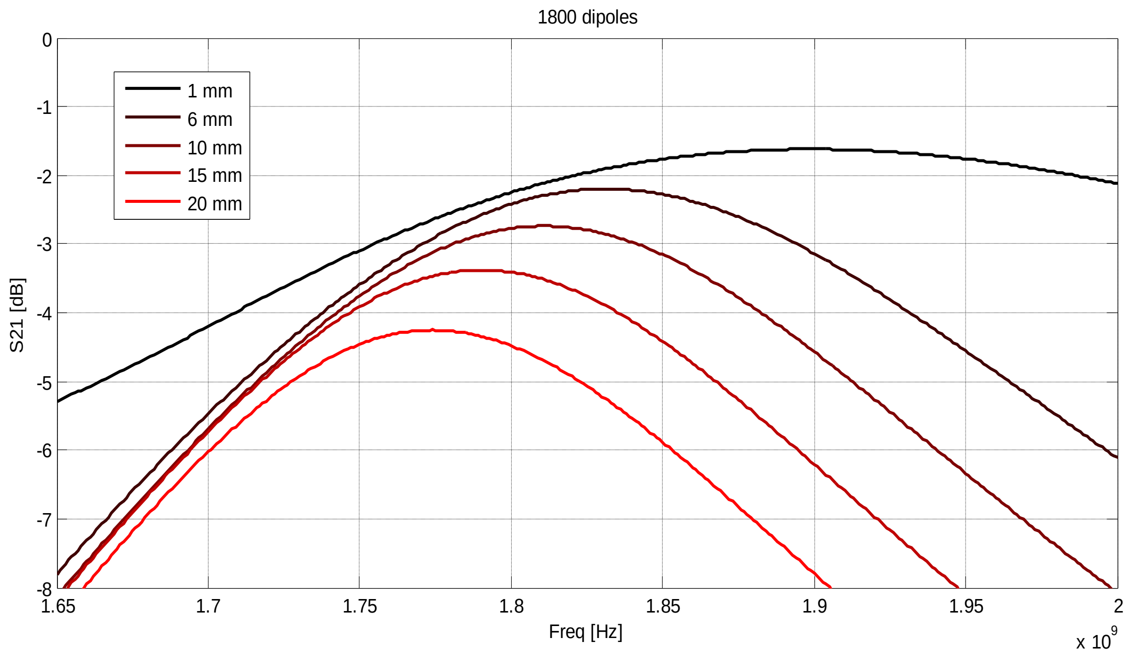


Figure 28: S21 dipoles 1800 MHz

- **One dipole at 900 MHz and the other at 1800 MHz separated d= 1mm, 6mm, 10mm, 15mm and 20 mm.**

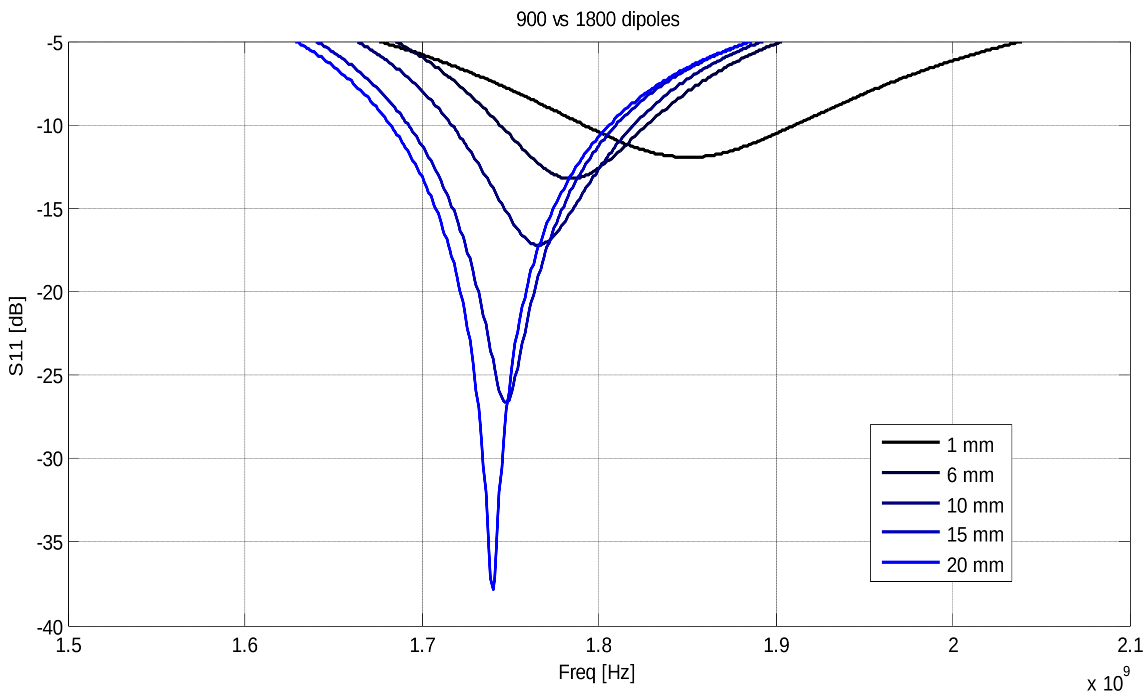


Figure 29: S11 dipoles 900 vs. 1800 MHz

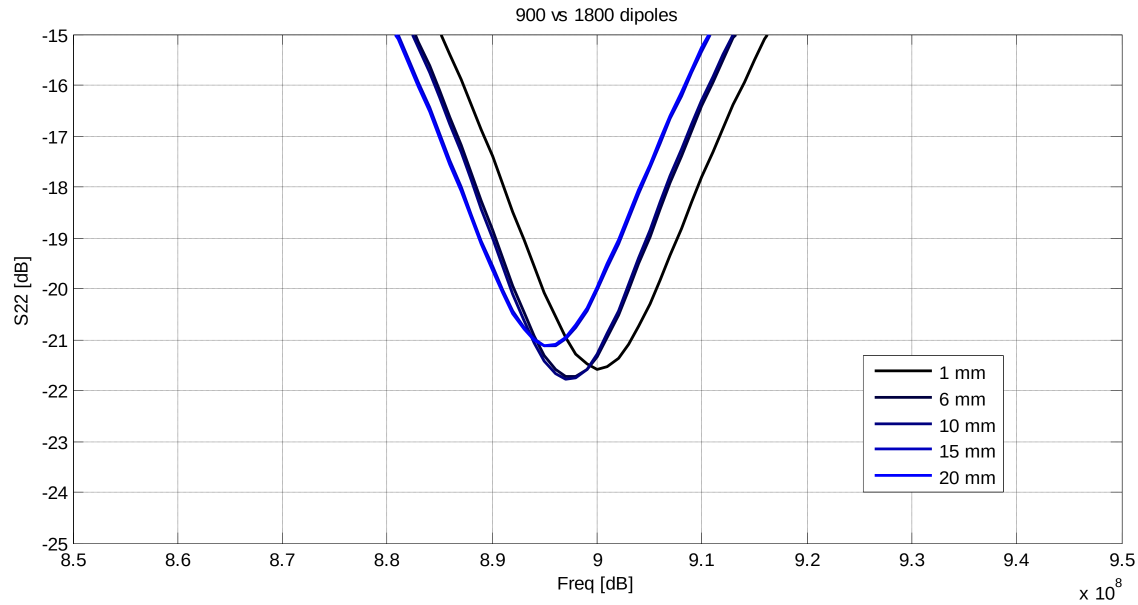


Figure 30: S22 dipoles 900 vs. 1800 MHz

We can notice that with higher separation between the dipoles, the closer it is to the designed frequency and it has better $S_{21}$. The following graph shows how $S_{21}$ changes.

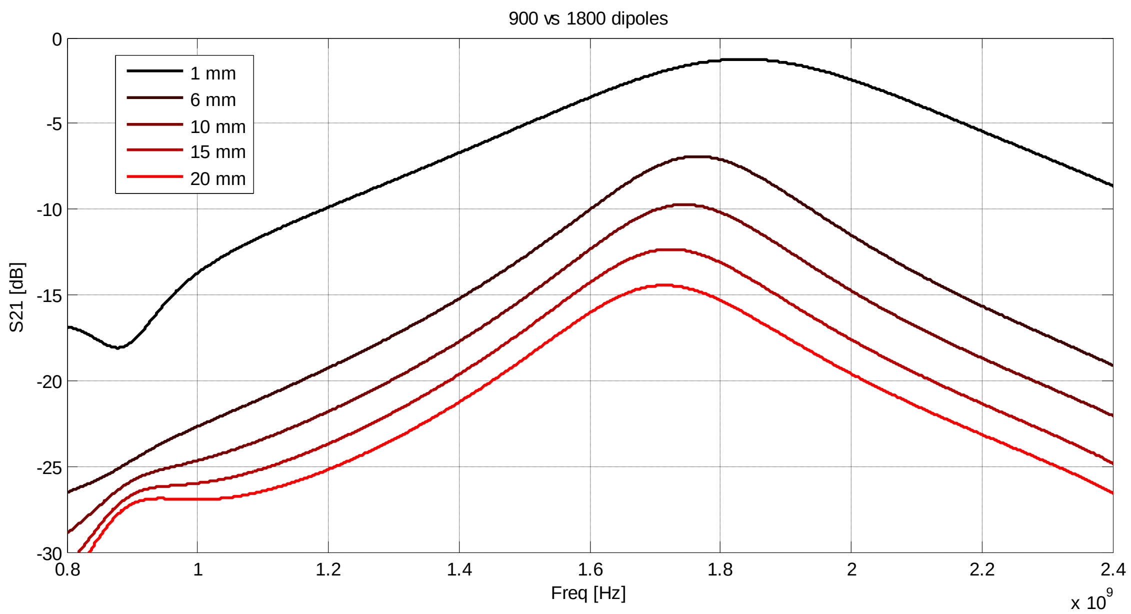


Figure 31: S22 dipoles 900 vs. 1800 MHz

# II. Two monopoles on ground plane (1800 MHz)

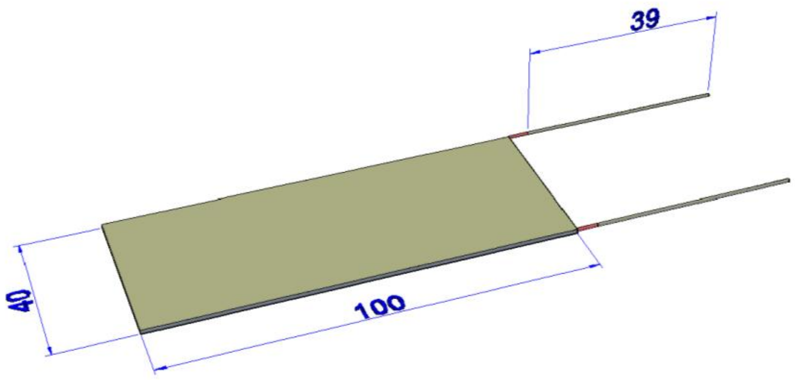


Figure 32: monopoles on PCB

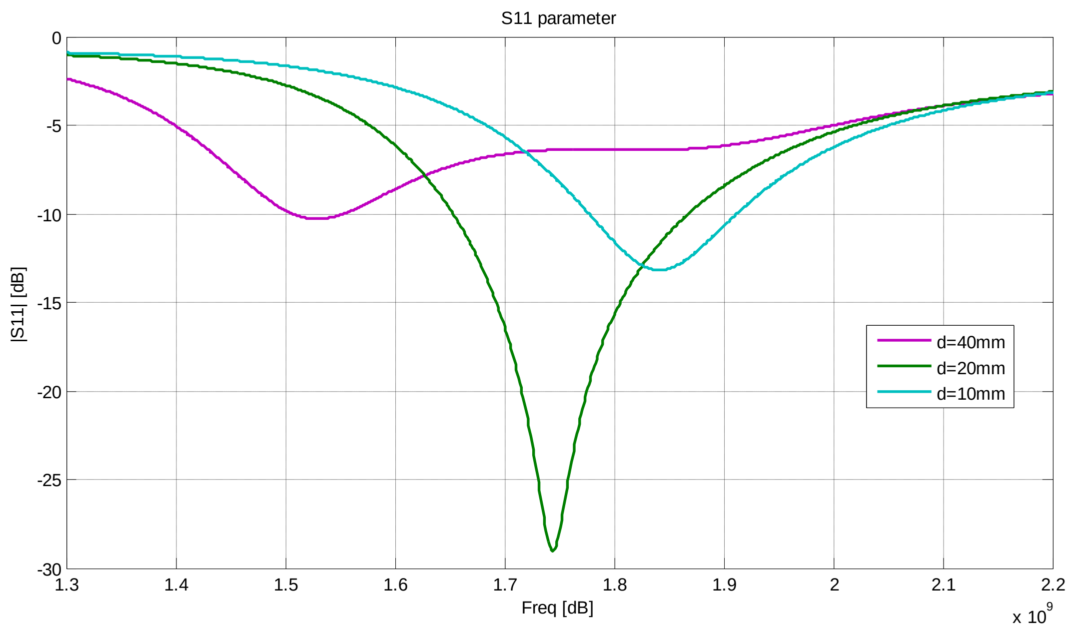


Figure 33: S11 monopoles 1800 MHz

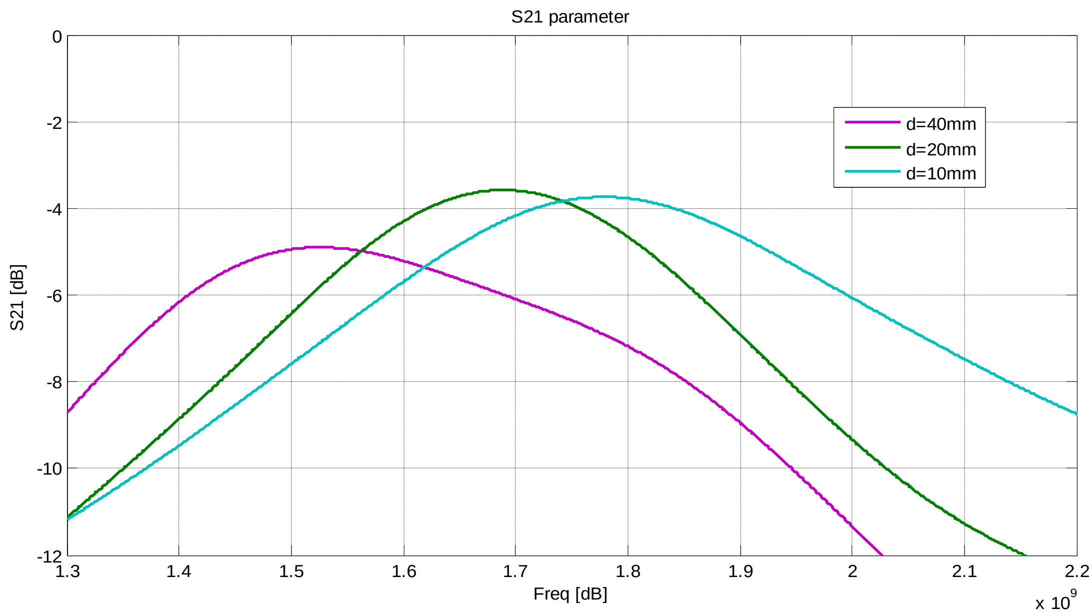


Figure 34: S22 monopoles 1800 MHz

# III. PIFAs

- **Different distance between feeding strip and short-circuit strip:**

In this part, we simulate a PIFA with different lengths between its feeding strip and its short-circuit strip, i.e. we give different values to *W*.

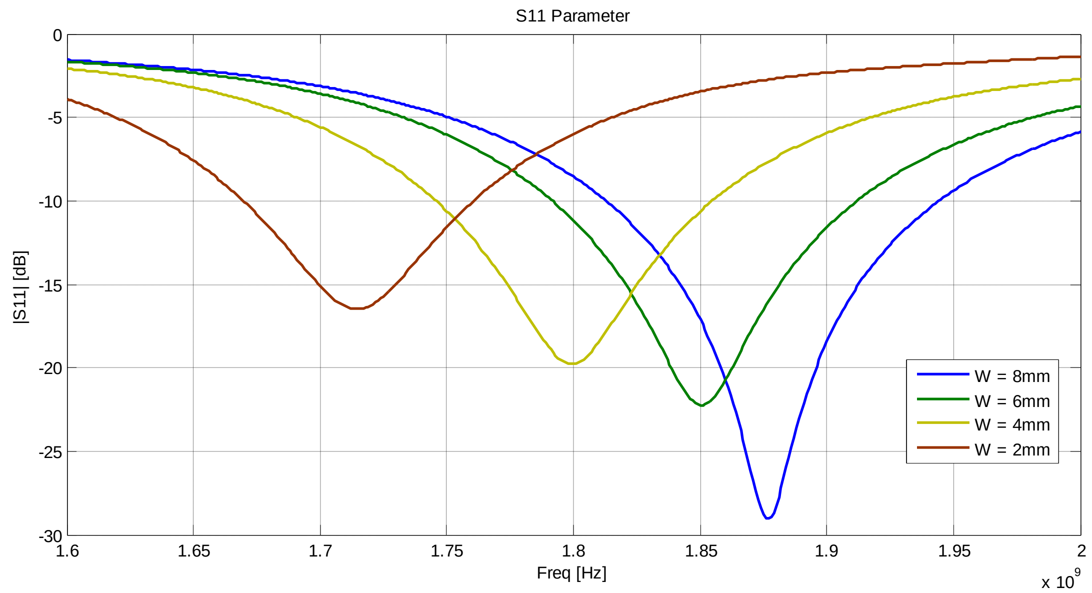


Figure 35: S11 vs. Different distance feeding & shorting strip

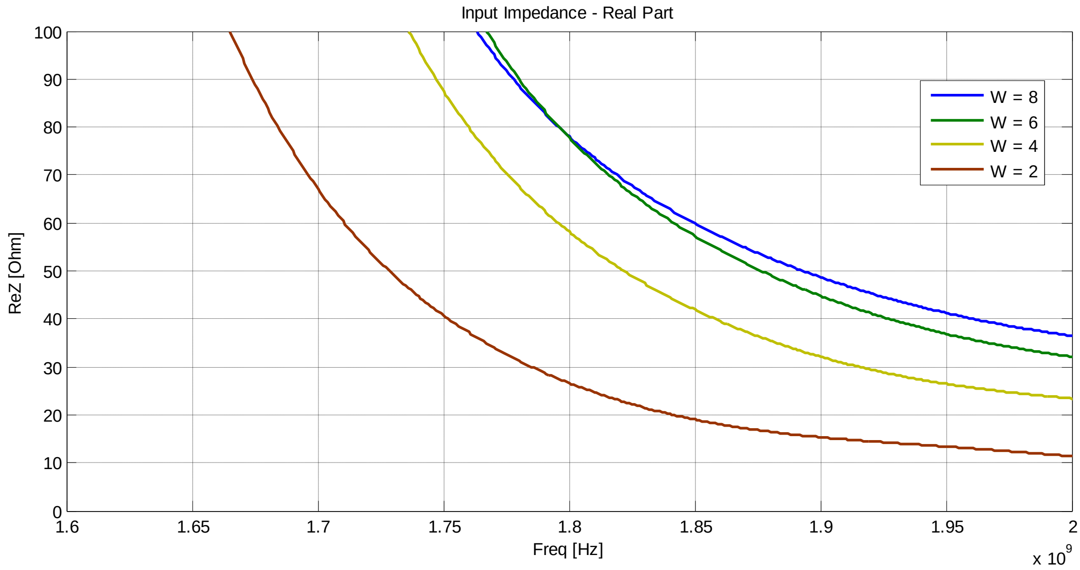


**Figure 36: Real part of impedance vs. distance feeding & shorting strip**

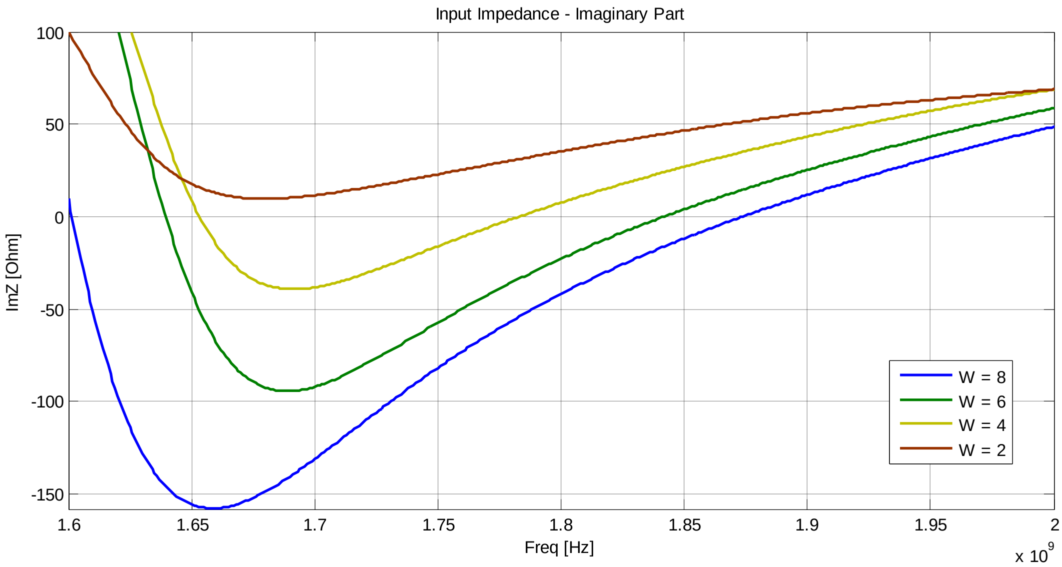


**Figure 37: Imaginary part of impedance vs. distance feeding & shorting strip**

- **Different heights**:

This figure represents the $\mathbf{S_{11}}$ for different heights "**H**" of a **PIFA of 26x8mm** with a separation **between feeding strip and short circuit strip "W" of 8mm**. This is important for the self-impedance.

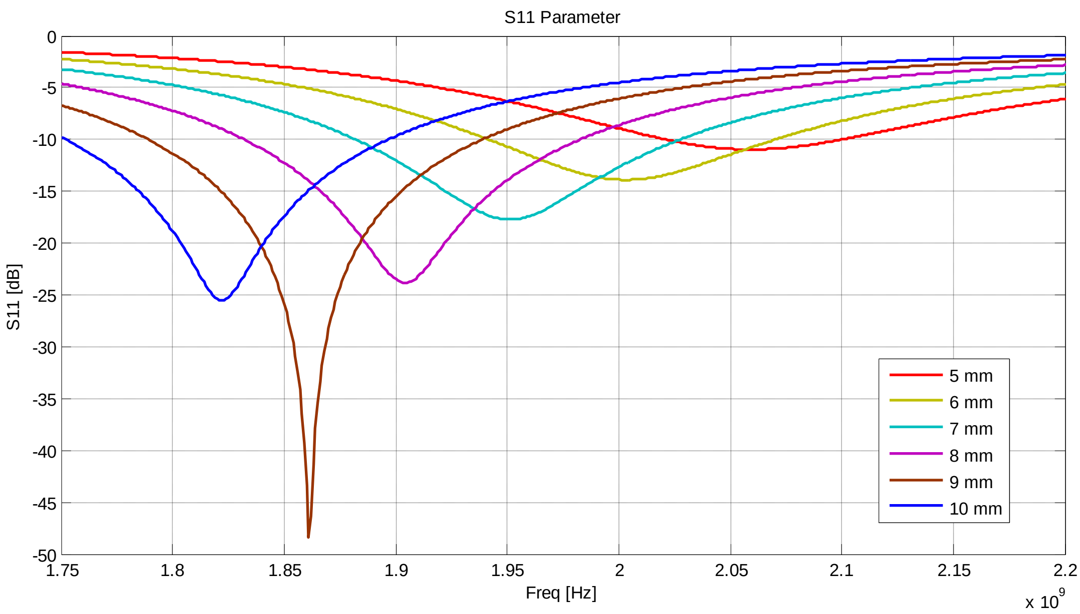


Figure 38: S11 vs. height of the PIFA from PCB

The rest of distances are not at the same level of $S_{11}$ because the antennas are not well matched, however we can see that the higher is the antenna the narrower is the bandwidth.

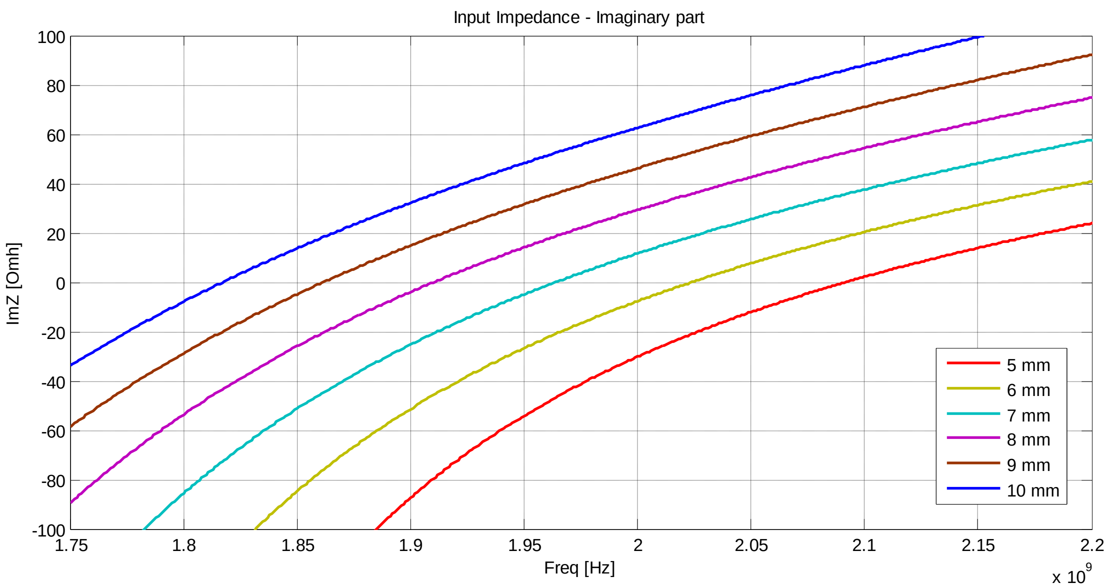


Figure 39: Impedance imaginary part vs. height of the PIFA from PCB

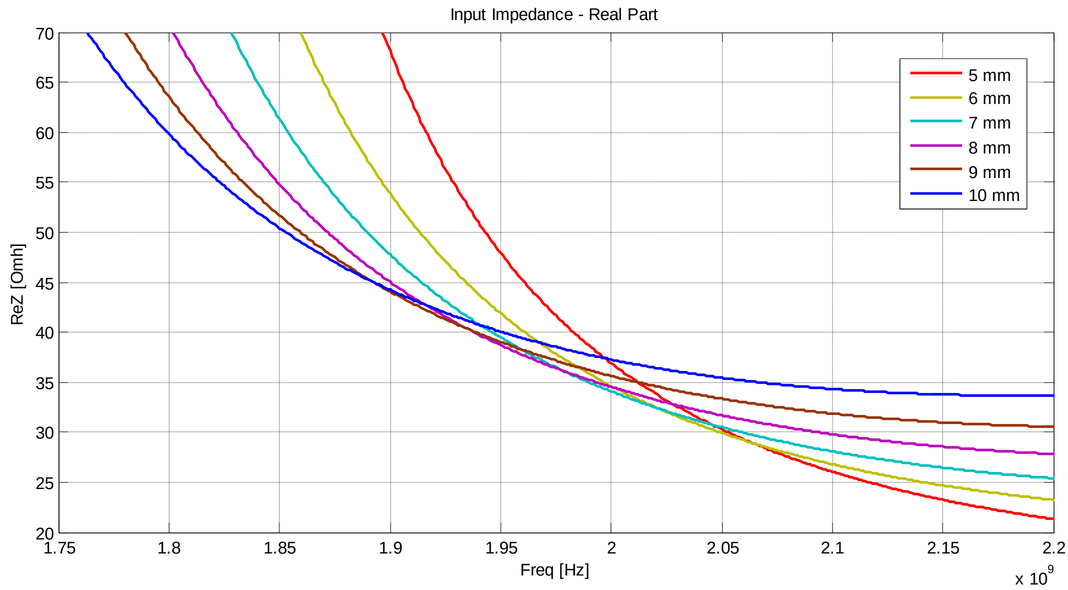


**Figure 40: Impedance real part vs. height of the PIFA from PCB**

- **Different distance between the PIFAs:**

PIFA is 26x8mm at a height "H" of 10 mm. Distance between feeding and shorting strip "W" is 8 mm.

➢ *Feed facing:*

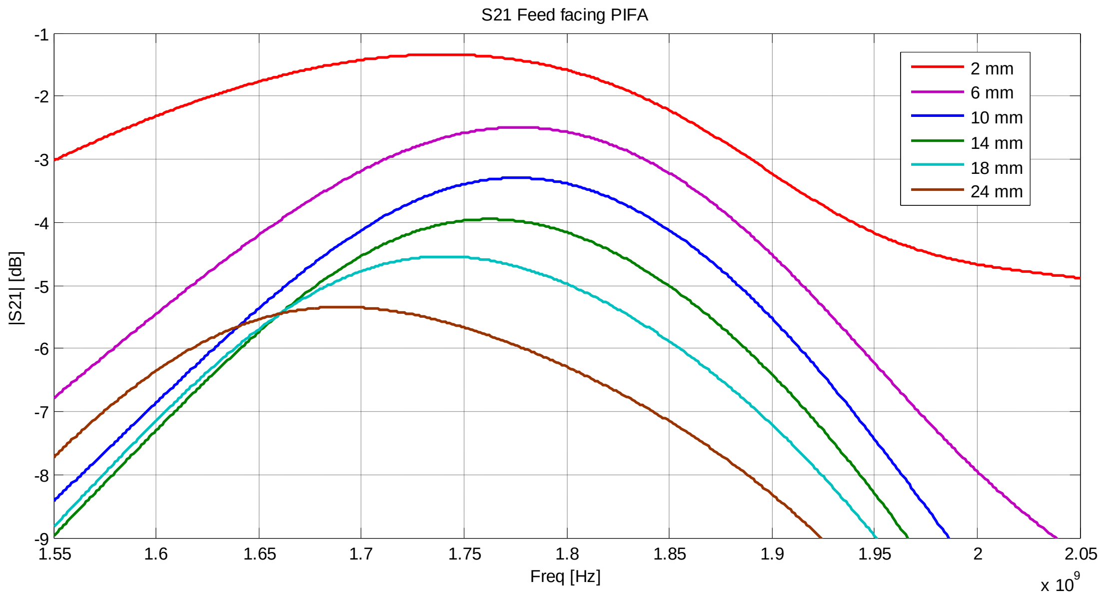


**Figure 41: S21 vs. distance between feed facing PIFAs**

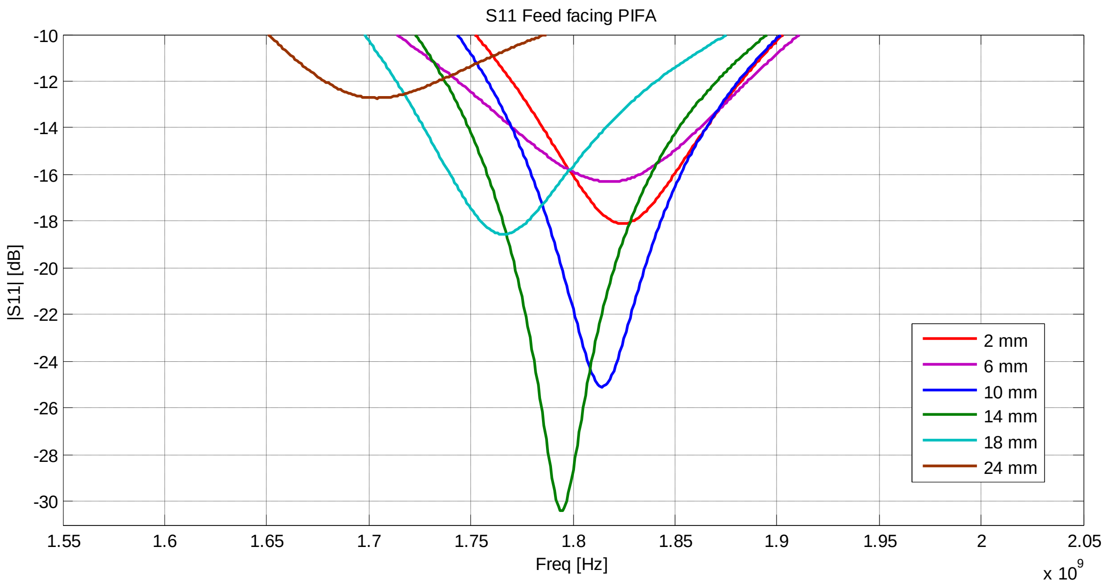


**Figure 42: S11 vs. distance between feed facing PIFAs**

- ***Short facing:***

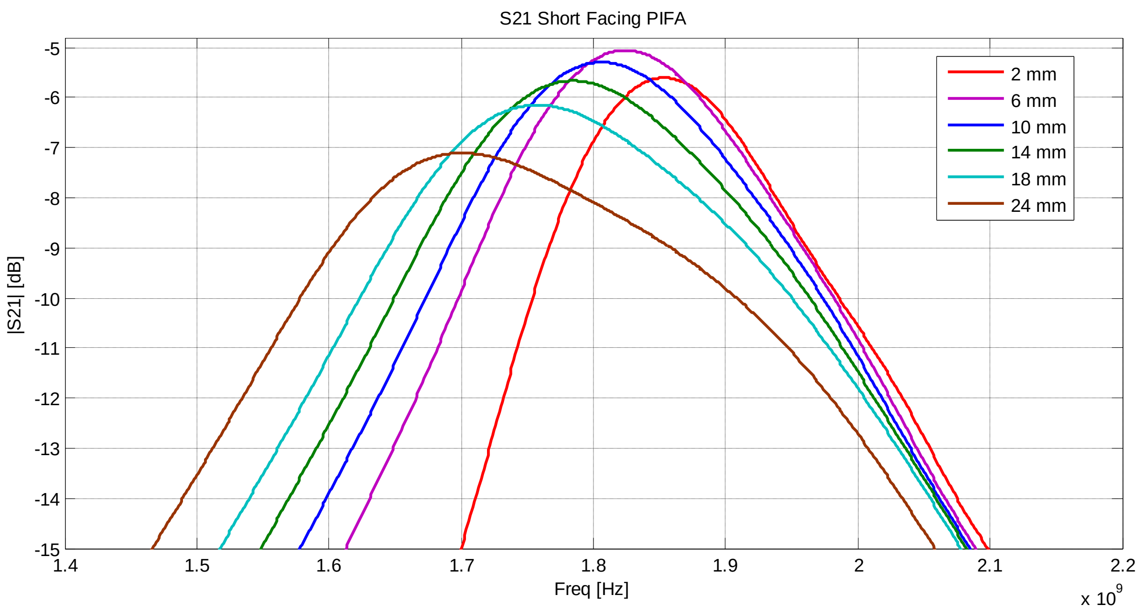


**Figure 43: S21 vs. distance between short facing PIFAs**

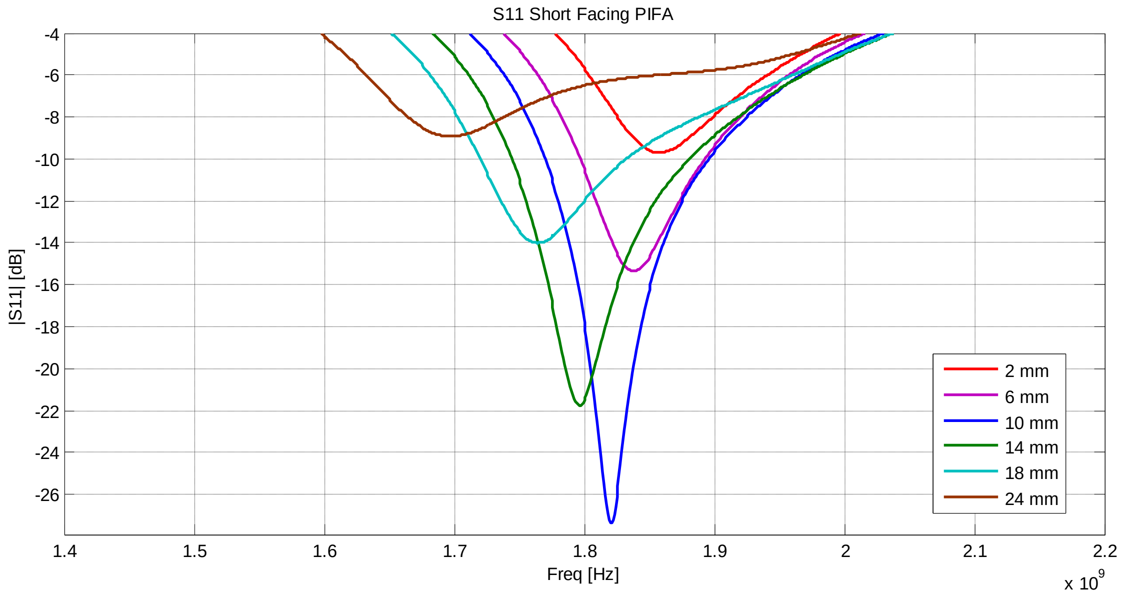


Figure 44: S11 vs. distance between short facing PIFAs

- ***PIFA GSM (880-960MHz):***

Due to the large dimension of a 900 MHz PIFA, it is recommended to use slots.

- L1=40 mm.
- L2=16 mm.
- W=4 mm.
- H =10 mm.
- Slot➔L1=2mm. & L2=1mm.

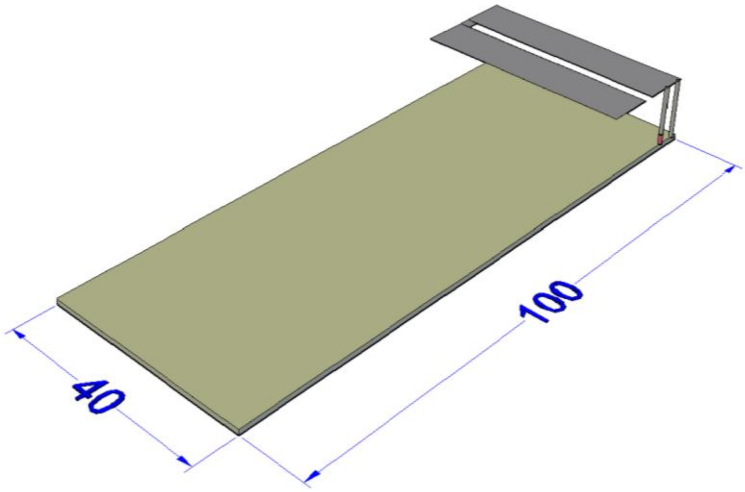


Figure 45: 900 MHz slot PIFA

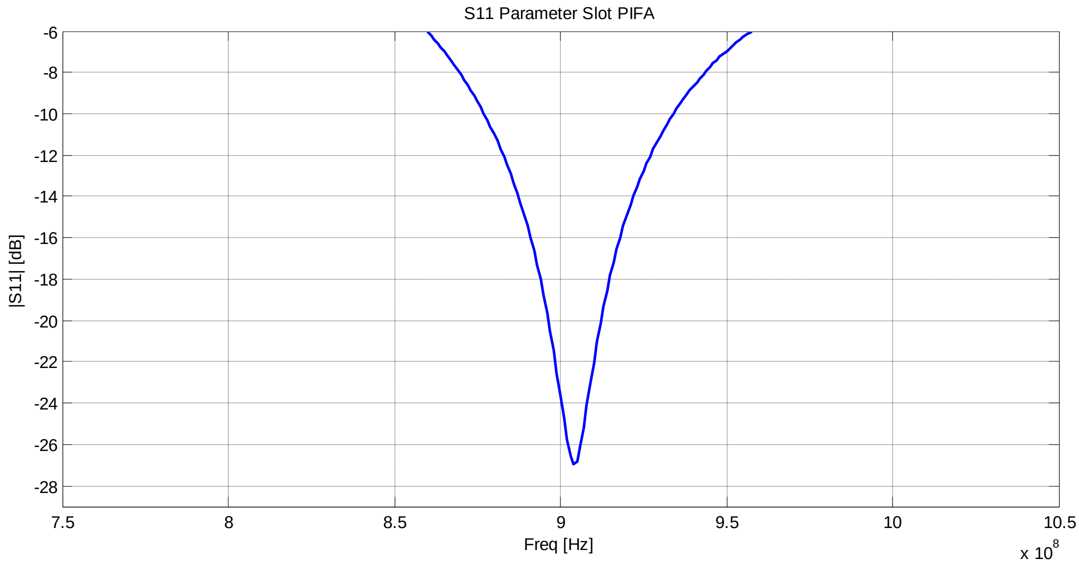


Figure 46: S11 of 900 MHz slot PIFA

*At **910 MHz** the impedance is 45.*

- **PIFA DCS(1710-1880MHz):**

The dimension of the **PIFA is 24x7mm. at a height "*H*" of 10 mm**. The distance between the short-circuit strip and the feeding strip "***W***" is 3mm.

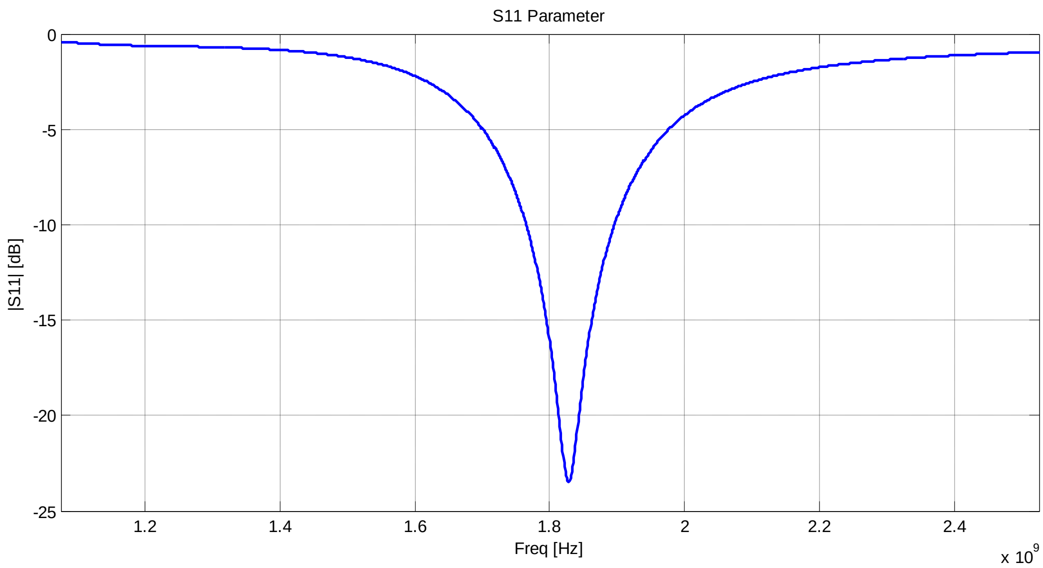


Figure 47: S11 of PIFA DCS

The resonance frequency is at 1.818 GHz and the impedance is 59 Ω.

- **Variation of two DCS PIFAs:**

  ➢ *Two PIFAs on top of the same PCB, edge to edge **spaced 24mm** from each other, as in below figure:*

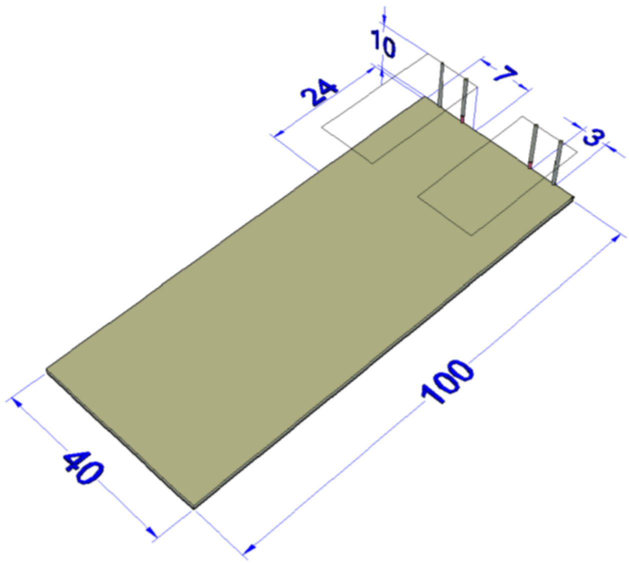


Figure 48: Two PIFAs (I)

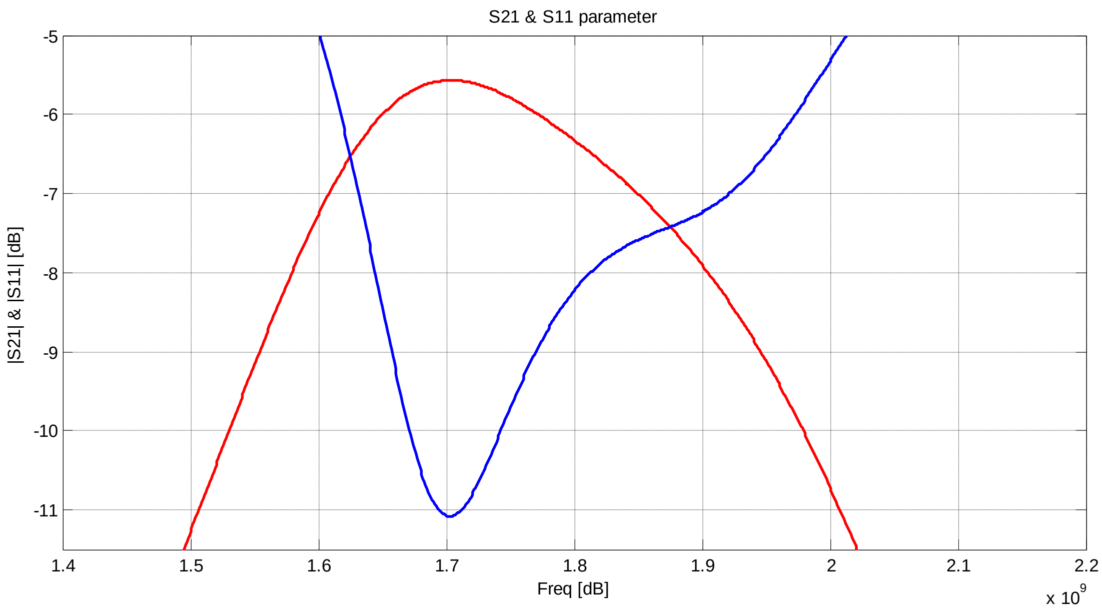


Figure 49: S11 & S21 of two PIFAs (I)

➢ *Two PIFAs with the same previous characteristics faced in front of each other as in figure.*

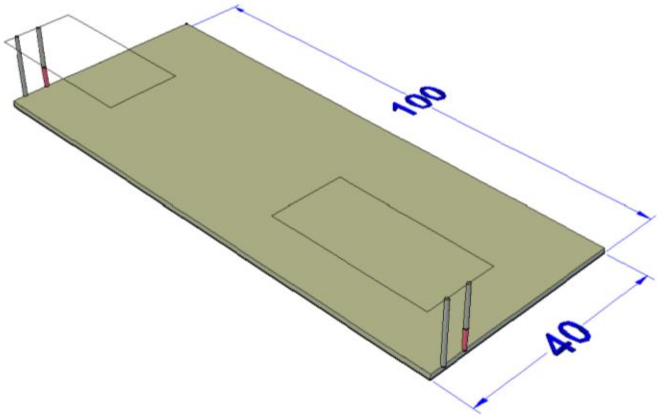


Figure 50: Two PIFAs (II)

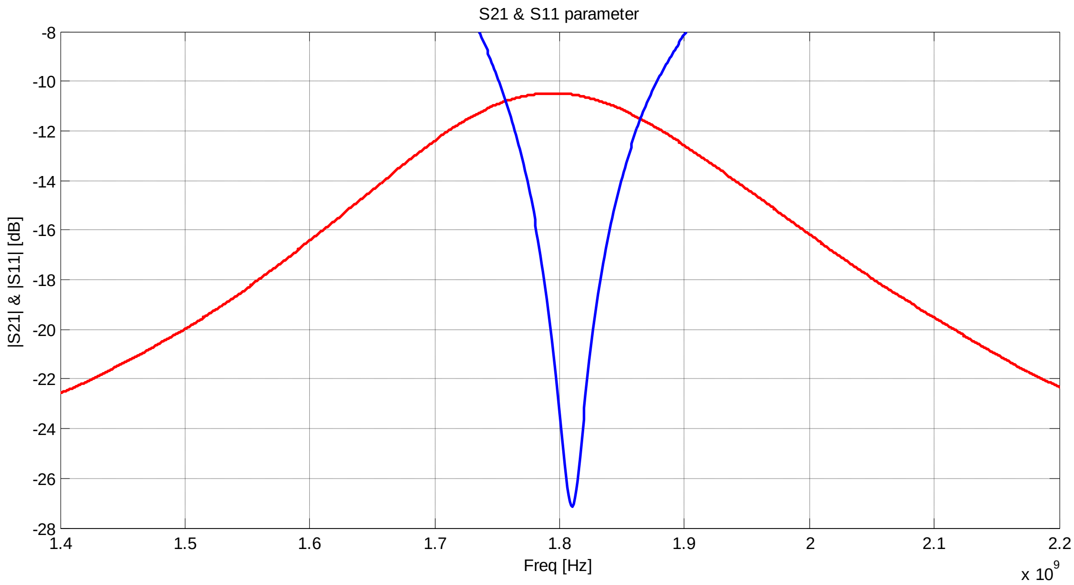


Figure 51: S11 & S21 of two PIFAs (II)

The $S_{11}$ is -27.13 dB and $S_{21}$ is -10.49 dB at frequency 1802MHz.

From the results obtained through the simulation, the real part of the impedance is 55.31Ω when it is at resonance frequency of 1804MHz.

➢ ***<u>Same PIFA characteristics but this time each PIFA is on the opposite edge of the ground plane with the source feeding towards the inside edges and not at the outside edges, such as shown in the following figure:</u>***

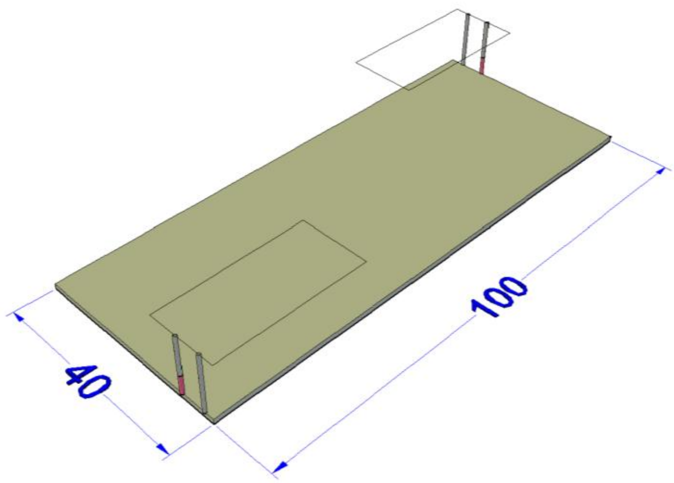


Figure 52: Two PIFAs (III)

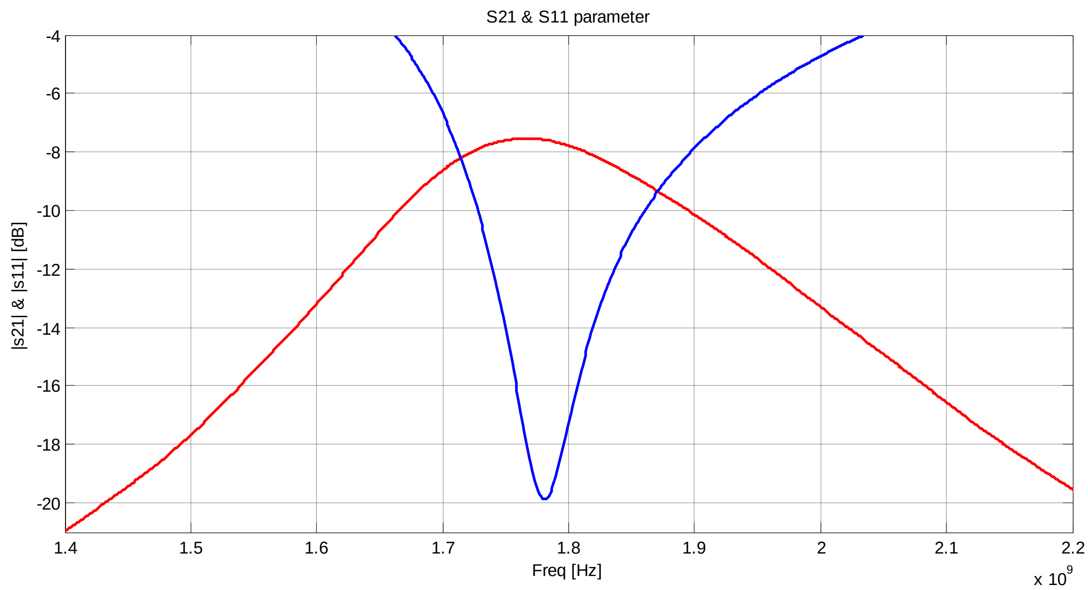


Figure 53: S11 & S21 of two PIFAs (III)

$S_{11}$ is -19.88dB and $S_{21}$ is -7.5dB at 1780MHz. The impedance at resonance frequency 1777MHz is 59.95Ω.

- ***<u>The first PIFA has the feeding strip on the inside edge and the second PIFA has the feeding strip on the outside edge. As in the following figure:</u>***

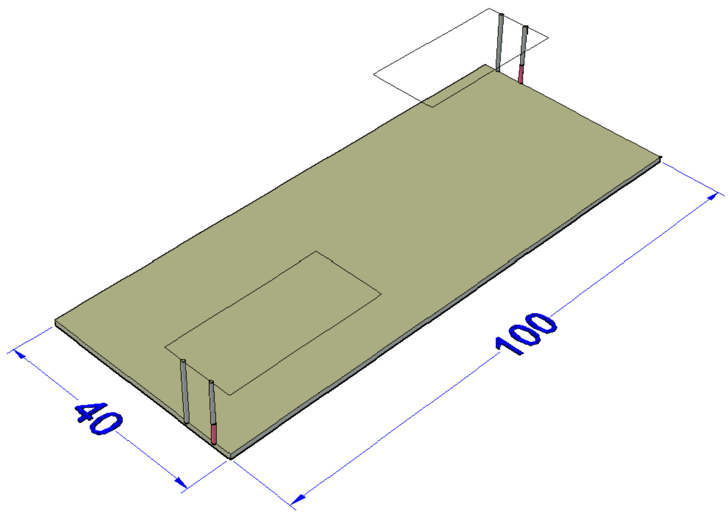


Figure 54: Two PIFAs (IV)

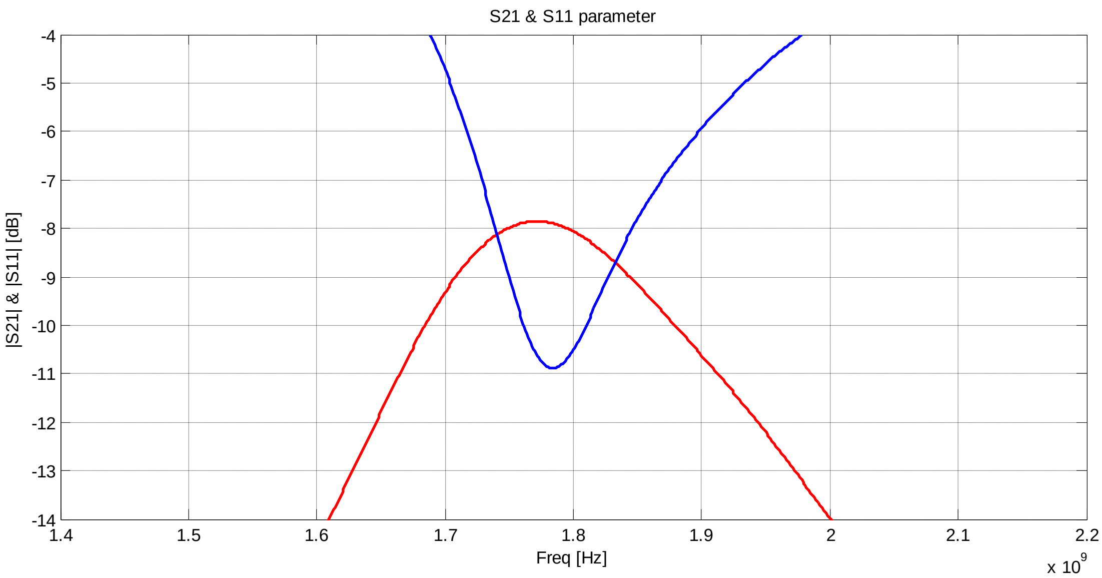


Figure 55: S11 & S21 of two PIFAs (IV)

$S_{11}$ is -10.88dB and $S_{21}$ is -7.9dB at 1786MHz. The impedance is 121Ω at resonance frequency1734 MHz. We clearly notice that we have matched the impedance.

➢ ***<u>Both PIFAs have their feeding strip on the outside edge.</u>***

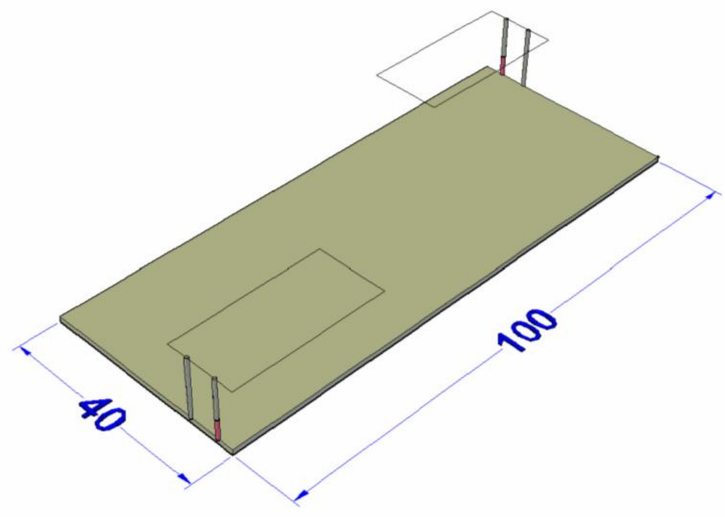


Figure 56: Two PIFAs (V)

From the graph below which represents the $S_{11}$ and $S_{21}$, we can that the $S_{11}$is around -10.86 dB and $S_{21}$ is around -7.8 dB at 1.78 MHz. The resonant frequency is 1.734 MHz and the real part is 121.5 Ω.

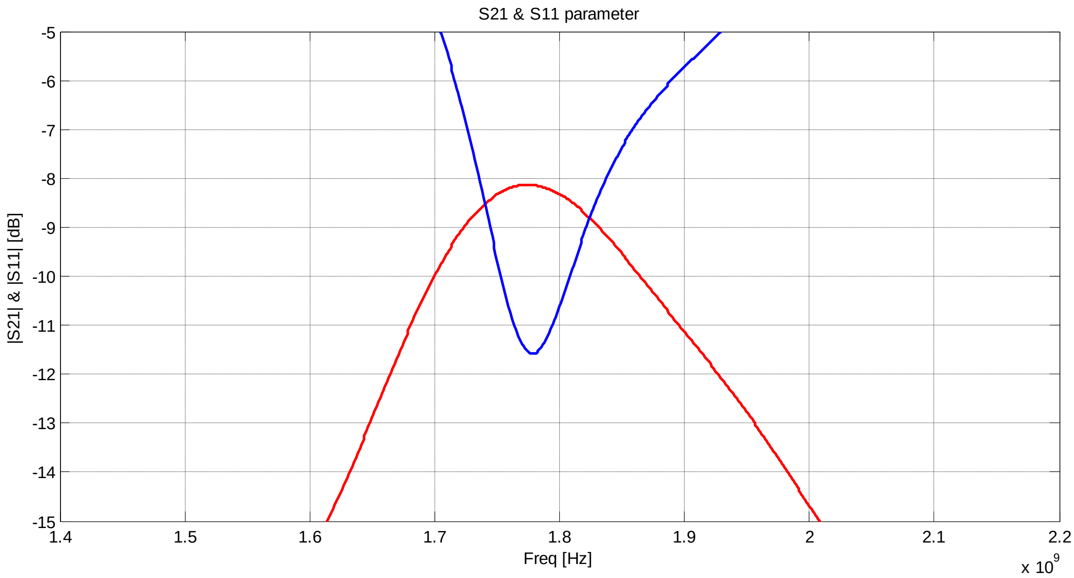


Figure 57: S11 & S21 of two PIFAs (V)

# IV. PIFAs with dielectric materials:

- **Two PIFAs feed facing with one dielectric wall in between:**
  1. DCS1800 ➔31x10 mm, H=10mm.
  2. UMTS➔27x8mm, H=10mm.

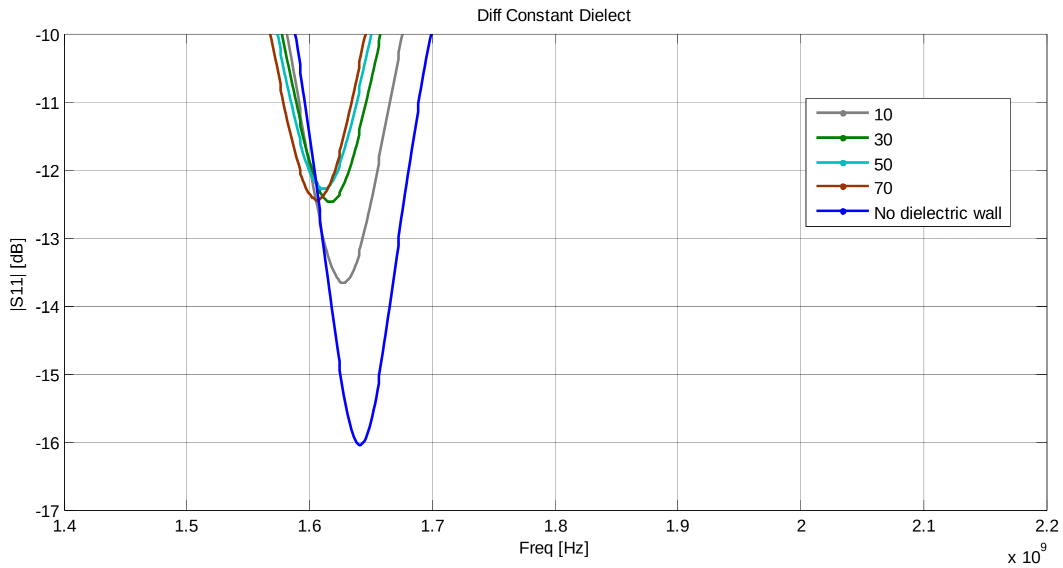


**Figure 58: S11 vs. different permittivity one wall**

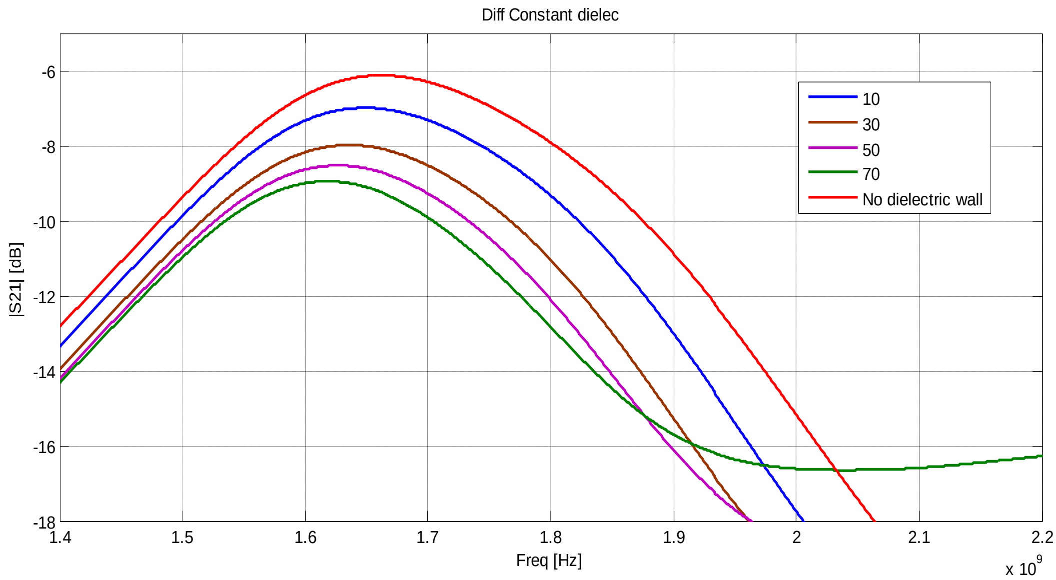


**Figure 59: S22 vs. different permittivity one wall**

- **PIFA with two dielectric walls**

  - *Vertical configuration*

| | S11 [dB] | S21 [dB] | S22 [dB] | η1 | η2 | MisLoss1 [dB] | MisLoss2 [dB] | ηtot1 | ηtot2 |
|---|---|---|---|---|---|---|---|---|---|
| Permittivity | | | | | | | | | |
| 100 | -20,60 | -19,87 | -31,12 | 0,956 | 0,95154 | 0,0379 | 0,0449 | 0,937 | 0,941 |
| 90 | -20,45 | -20,50 | -29,58 | 0,958 | 0,95399 | 0,0393 | 0,0388 | 0,941 | 0,944 |
| 80 | -20,54 | -19,74 | -27,74 | 0,961 | 0,95225 | 0,0385 | 0,0463 | 0,942 | 0,940 |
| 70 | -20,87 | -18,90 | -25,75 | 0,962 | 0,94650 | 0,0356 | 0,0563 | 0,942 | 0,931 |
| 60 | -21,50 | -18,03 | -23,67 | 0,962 | 0,93709 | 0,0308 | 0,0689 | 0,940 | 0,918 |
| 50 | -22,54 | -17,15 | -21,54 | 0,962 | 0,92414 | 0,0242 | 0,0845 | 0,938 | 0,899 |
| No dielec | -21,89 | -7,890 | -15,33 | 0,780 | 0,90870 | 0,0281 | 0,7704 | 0,648 | 0,734 |

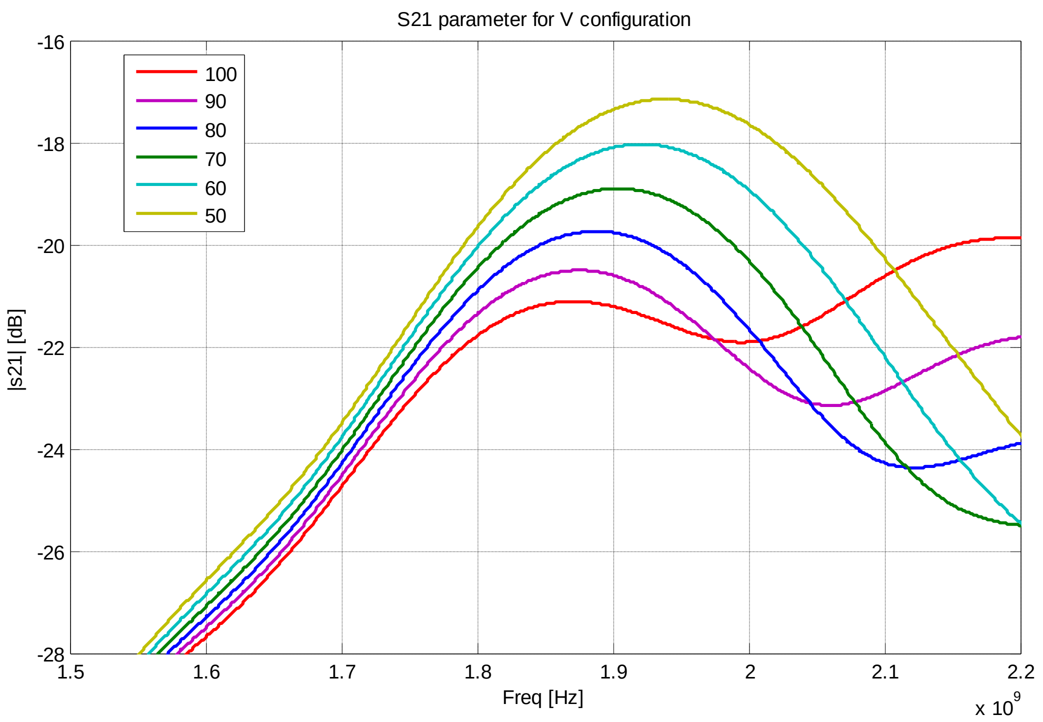


Figure 60: S21 vs. different permittivity two walls (V configuration)

- *Horizontal configuration*

| | *S11 [dB]* | *S21 [dB]* | *S22 [dB]* | *η1* | *η2* | *MisLoss1 [dB]* | *MisLoss2 [dB]* | *ηtot1* | *ηtot2* |
|---|---|---|---|---|---|---|---|---|---|
| 100 | -18,45 | -18,20 | -32,93 | 0,980 | 0,958 | 0,0625 | 0,0662 | 0,951 | 0,943 |
| 90 | -18,80 | -18,20 | -38,93 | 0,977 | 0,960 | 0,0576 | 0,0662 | 0,949 | 0,945 |
| 80 | -19,28 | -18,20 | -53,23 | 0,970 | 0,960 | 0,0515 | 0,0662 | 0,943 | 0,945 |
| 70 | -19,92 | -18,18 | -35,07 | 0,960 | 0,959 | 0,0444 | 0,0665 | 0,935 | 0,944 |
| 60 | -20,83 | -18,16 | -28,89 | 0,955 | 0,956 | 0,0360 | 0,0668 | 0,932 | 0,941 |
| 50 | -22,17 | -18,14 | -24,73 | 0,950 | 0,953 | 0,0264 | 0,0671 | 0,929 | 0,935 |
| No diele | -14,95 | -10,06 | -26,49 | 0,890 | 0,953 | 0,1411 | 0,4509 | 0,773 | 0,857 |

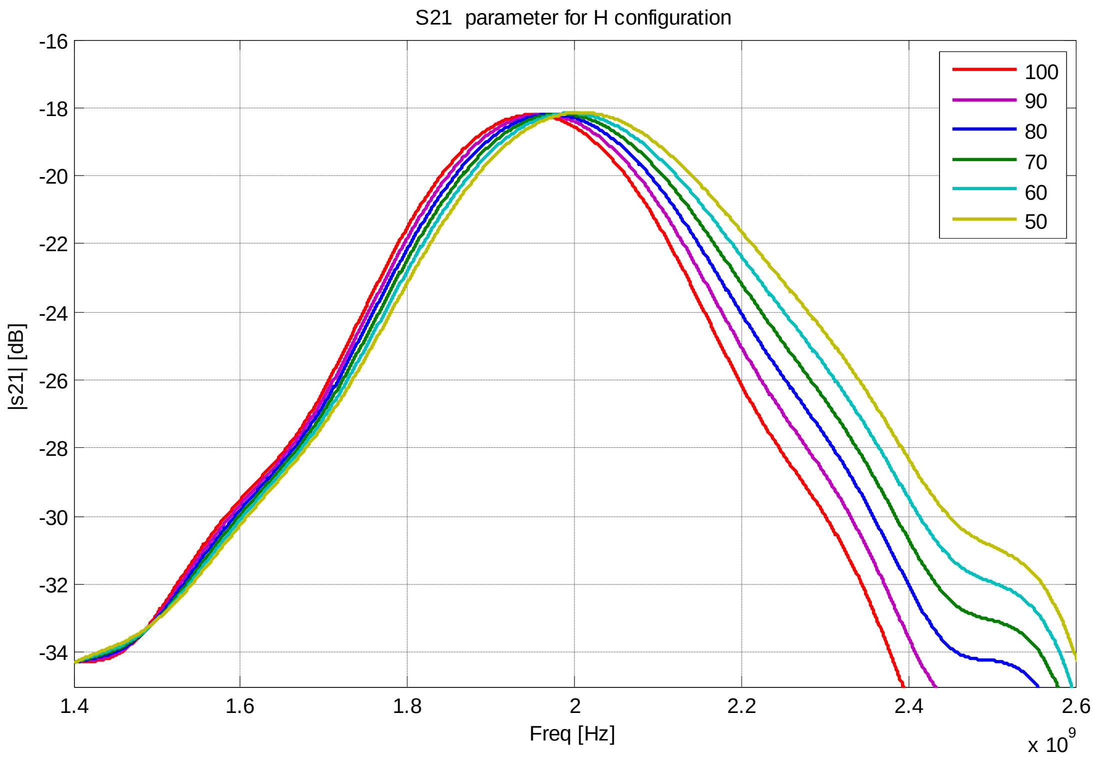


**Figure 61: S21 vs. different permittivity two walls (H configuration)**

- **Dielectric with Hands**

  - *Vertical configuration*

| Hands | S11 [dB] | S21 [dB] | S22 [dB] | $\eta1$ | $\eta2$ | MisLoss1 [dB] | MisLoss2 [dB] | $\eta tot1$ | $\eta tot2$ |
|---|---|---|---|---|---|---|---|---|---|
| h1 | -10,44 | -19,49 | -20,54 | 0,3716 | 0,61352 | 0,4113 | 0,0491 | 0,333 | 0,601 |
| h2 | -31,22 | -16,87 | -20,06 | 0,4760 | 0,49550 | 0,0032 | 0,0902 | 0,465 | 0,480 |
| h3 | -22,13 | -15,27 | -10,54 | 0,6490 | 0,35301 | 0,0266 | 0,1310 | 0,625 | 0,311 |
| h4 | -11,20 | -19,19 | -18,73 | 0,4348 | 0,60200 | 0,3426 | 0,0526 | 0,396 | 0,586 |
| h5 | -38,20 | -16,13 | -22,21 | 0,5531 | 0,48600 | 0,0006 | 0,1071 | 0,539 | 0,471 |
| h6 | -25,87 | -18,03 | -9,56 | 0,6341 | 0,40687 | 0,0112 | 0,0689 | 0,622 | 0,355 |

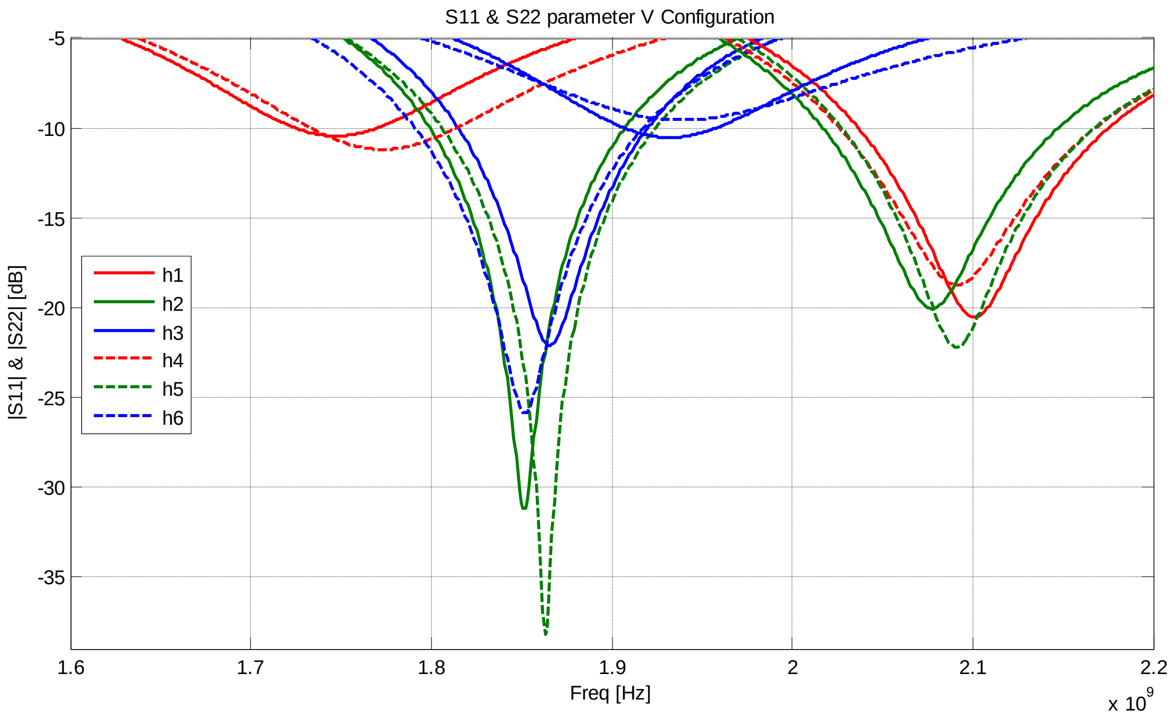


Figure 62: S11 & S22 vs. different hands (two walls V configuration)

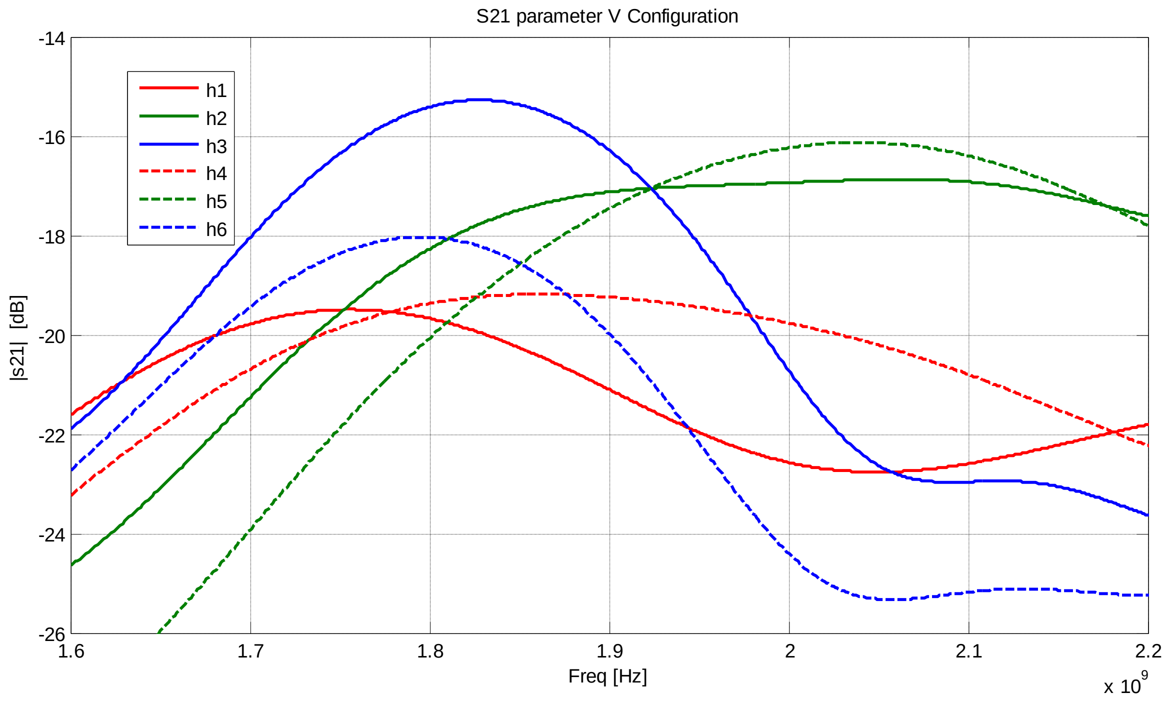


**Figure 63: S21 vs. different hands (two walls V configuration)**

- *Horizontal configuration*

| *Hands* | *S11 [dB]* | *S21 [dB]* | *S22 [dB]* | *η1* | *η2* | *MisLoss1 [dB]* | *MisLoss2 [dB]* | *ηtot1* | *ηtot2* |
|---|---|---|---|---|---|---|---|---|---|
| h1 | -26,77 | -13,02 | -10,83 | 0,4336 | 0,3057 | 0,0091 | 0,2222 | 0,4110 | 0,2652 |
| h2 | -24,83 | -13,12 | -11,31 | 0,4850 | 0,3072 | 0,0143 | 0,2170 | 0,4597 | 0,2695 |
| h3 | -16,51 | -15,75 | -11,54 | 0,6640 | 0,3680 | 0,0981 | 0,1171 | 0,6315 | 0,3323 |
| h4 | -17,17 | -21,16 | -21,96 | 0,4923 | 0,4970 | 0,0841 | 0,0333 | 0,4790 | 0,4900 |
| h5 | -33,62 | -20,96 | -19,71 | 0,5320 | 0,4817 | 0,0018 | 0,0349 | 0,5275 | 0,4727 |
| h6 | -18,51 | -22,00 | -20,95 | 0,6680 | 0,4898 | 0,0616 | 0,0274 | 0,6543 | 0,4828 |

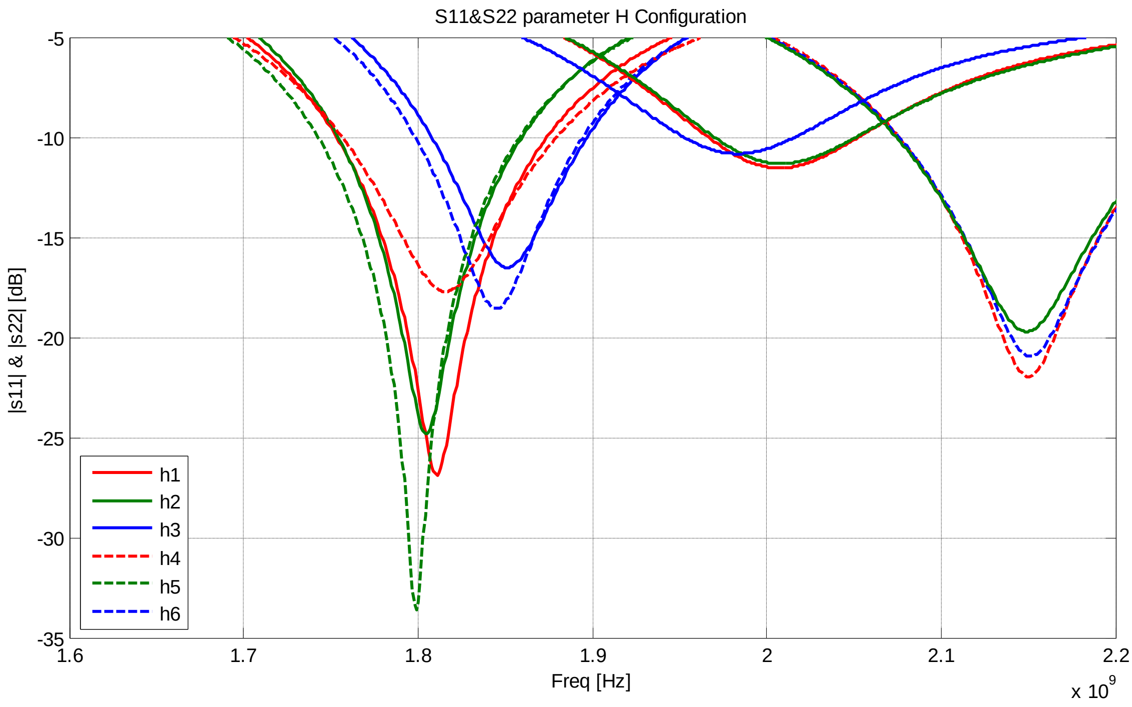


Figure 64: S11 & S22 vs. different hands (two walls H configuration)

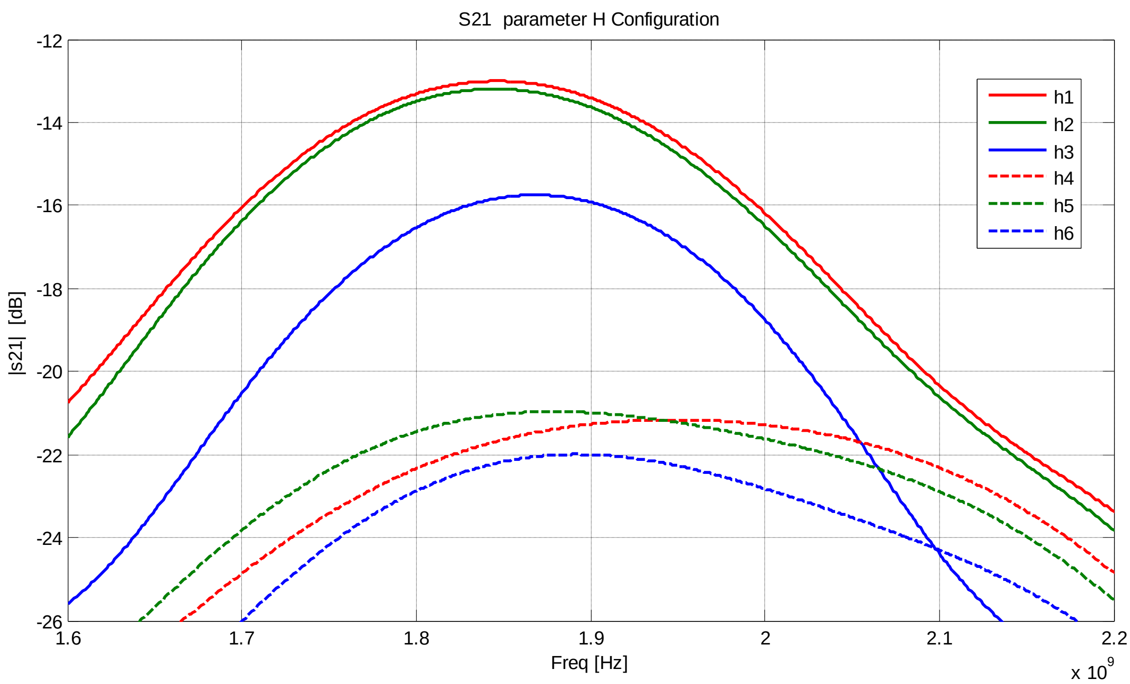


Figure 65: S21 vs. different hands (two walls H configuration)

# Appendix C. Hands

## I. Hand with Vertical Configuration

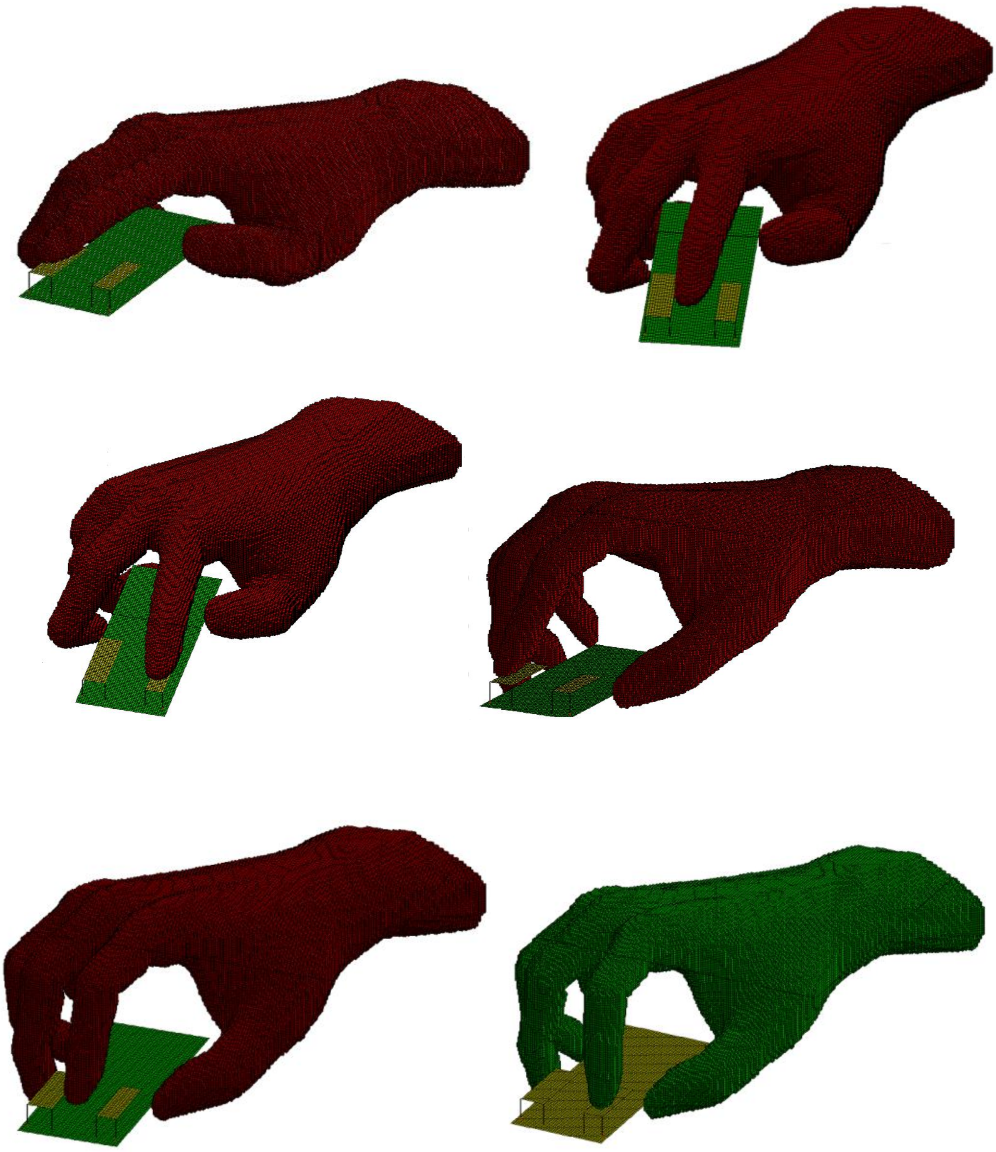

Figure 66: Hands Models V configuration (left h1, h3, h5) (right h2, h4, h6)

# II. Hands with Horizontal Configuration

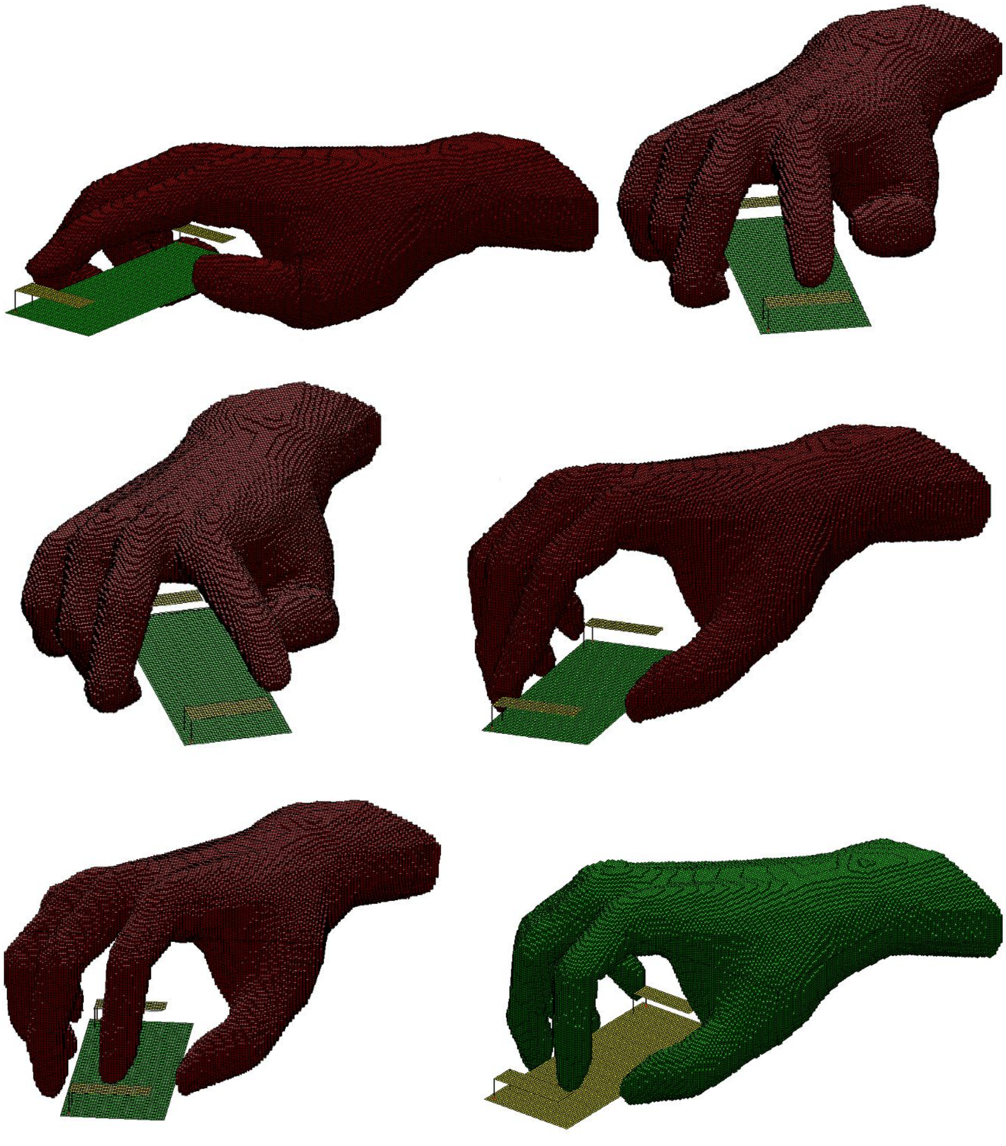

Figure 67: Hands Models H configuration (left h1, h3, h5) (right h2, h4, h6)

# Appendix D. Paper

***Study and Reduction of the Mutual Coupling between Two Mobile Phone PIFAs Operating in the DCS1800 and UMTS Bands*** [6]*:*

Here the width and the length of the wire have found to affect on the **$S_{21}$** curves, therefore we will demonstrate and understand what is done by simulating the proposed design.

Due to that our programme is limited in drawing the sizes; we will just change a bit the measurements. The abstract used a Digital Cellular Service antenna “DCS1800” of 30.5x10 mm and we used 31x10 mm. The other antenna was a Universal Mobile Telecommunications System “UMTS” antenna of 26.7x8mm and we used 27x8mm. instead. In this case we used a cell size of 1mm to have a wire of 1mm.

- Antenna DCS: L1=31mm, L2=10mm, H=9 mm and W=10mm.
- Antenna UMTS: L1=27mm, L2=8mm, H=9mm and W=8mm.

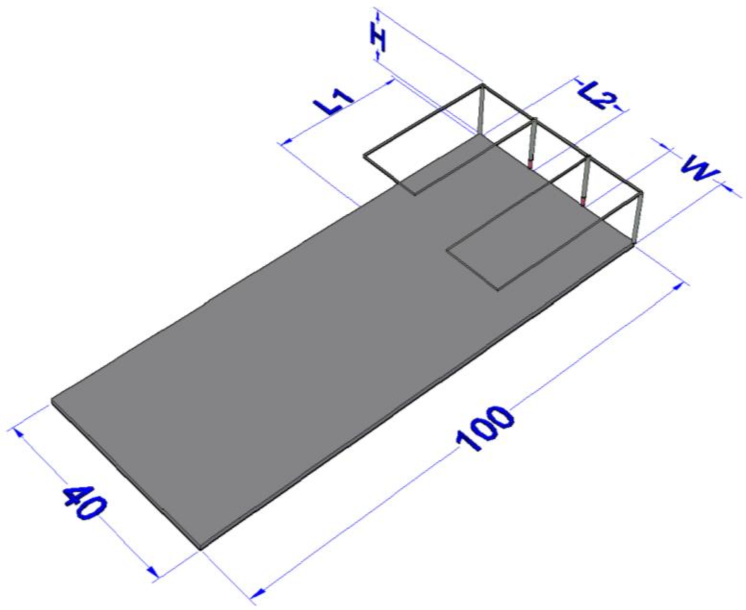


**Figure 68: Line between PIFAs**

Our results of $S_{21}$ and $S_{11}$ without any transmission line in between with **shorting strips facing** are:

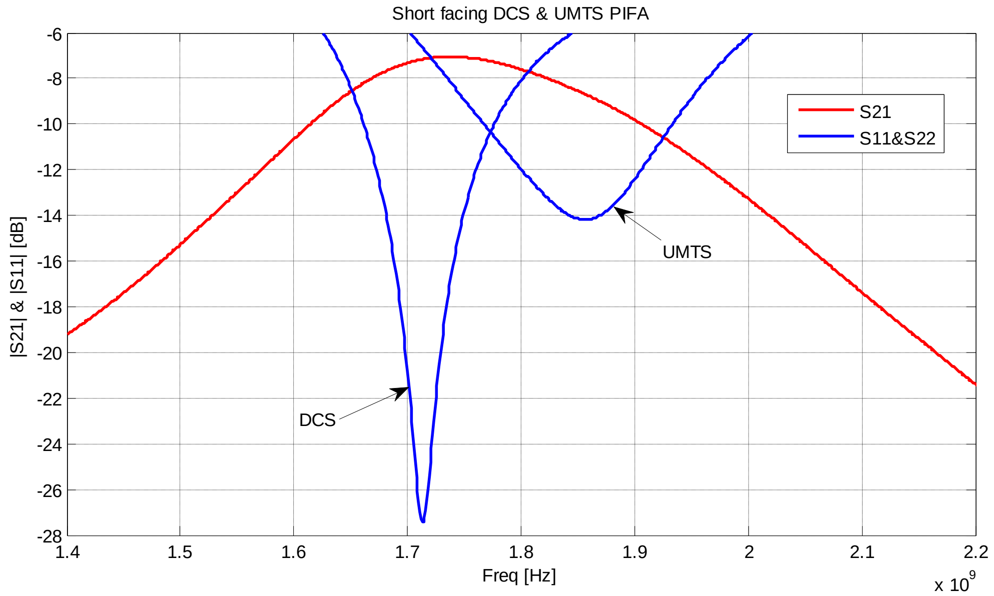


Figure 69: S21 and S11 without any transmission line

- **Antennas with line:**

We inserted a transmission line between the **shorting** of both antennas. We did the simulation for different widths of transmission lines.

For a wire of **1mm** width we obtained the following:

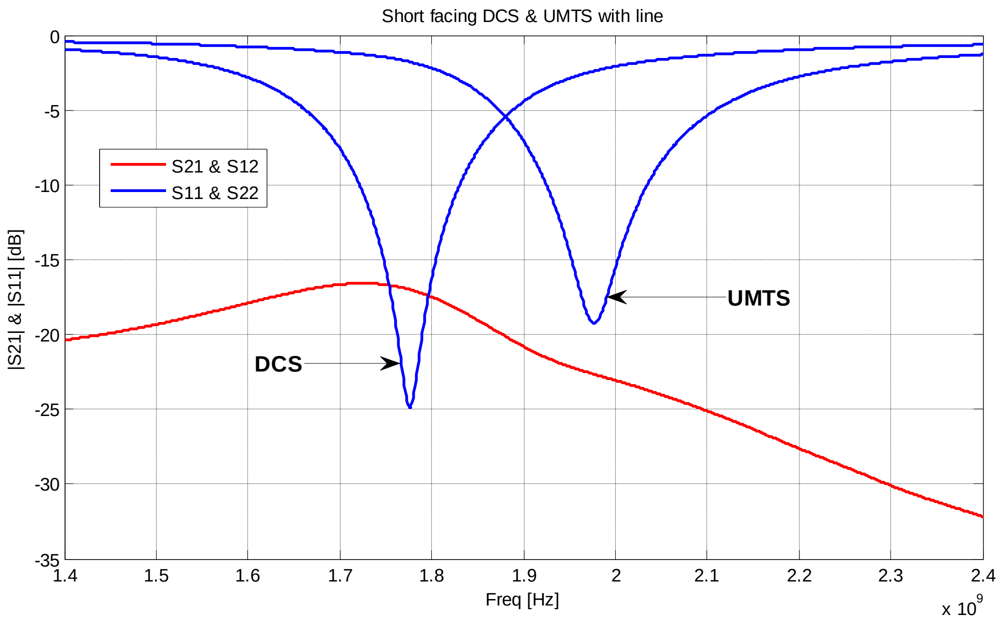


Figure 70: S21 and S11 with transmission line 1 mm

For a wire of **0.5mm** width we obtained the following:

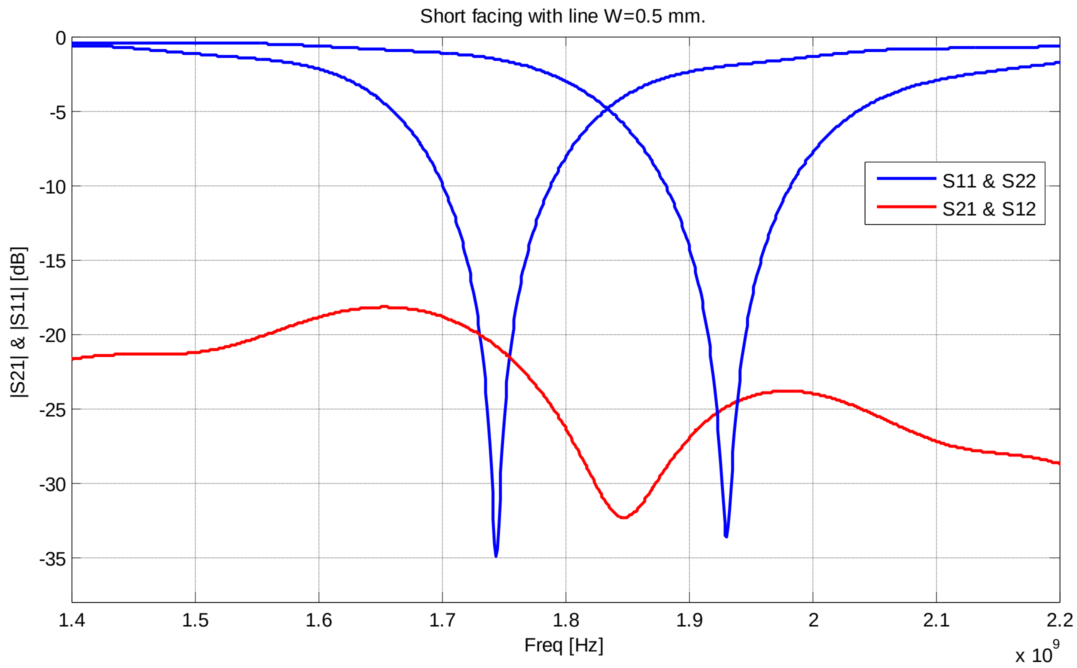


Figure 71: S21 and S11 with transmission line 0.5mm